Smectic A Mesophases from Luminescent Sandic Platinum(II) Mesogens

Note: The following files were submitted by the author for peer review, but cannot be converted to PDF. You must view these files (e.g. movies) online.

PtC6.cif
PtC8.cif
PtC12B.cif

SCHOLARONE™
Manuscripts
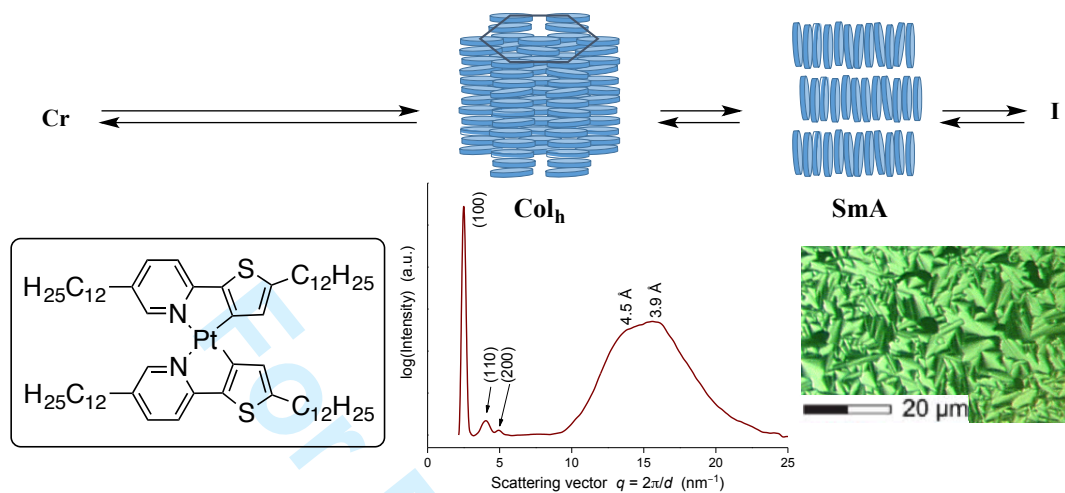
Smectic A Mesophases from Luminescent Sandic Platinum(II) Mesogens

Markrete Krikorian,[§a] Constantin-Christian A. Voll,[§a] Maryam Yoon,[a] Koushik Venkatesan,[*b] Paul H. J. Kouwer,[*c] and Timothy M. Swager[*a]

[a]Department of Chemistry, Massachusetts Institute of Chemistry, Cambridge, Massachusetts 02139, United States. Email: tswager@mit.edu

[b]Department of Chemistry, University of Zürich, 8057 Zürich, Switzerland. Email: venkatesan.koushik@chem.uzh.ch

[c]Institute for Molecules and Materials, Radboud University Nijmegen, Heyendaalseweg 135, 6525 AJ Nijmegen, The Netherlands. Email: p.kouwer@science.ru.nl

[§]These authors contributed equally to the manuscript.

Smectic A Mesophases from Luminescent Sandic Platinum(II) Mesogens

Square planar platinum(II) thienyl pyridyl complexes with board-shaped structures assemble into lamellar (SmA) liquid crystal phases at elevated temperatures. Liquid crystals of this type are expected to have stronger biaxial correlations than typical calamitic mesogens. The mesophase stability improves with decreasing alkyl chain lengths with C_8H_{17} having the widest range of stability. All complexes are luminescent in solution.

Keywords: Pt(II); sandic; SmA, Col_h

1. Introduction

The tunable assembly of molecules into bulk materials by the facile manipulation of structural components is of central interest to materials chemists.[1–3] Third row transition metal complexes are particularly useful building blocks and have played an essential role in devices including light emitting diodes,[4,5] photovoltaic cells,[6] sensors,[7,8] polarized electroluminescent devices,[9–11] and field effect transistors.[11] These complexes often serve as dopants or secondary components[12] in established and emerging systems [6,13-16a]. Strong luminescence and absorption in the visible region of some third row transition metal complexes make them appealing candidates for electrooptical devices.[16b-d] Endowing functional molecular building blocks with structural components that encourage liquid crystallinity, and the bulk organizations produced therein, has often expanded their utility and applications. [11] Towards this end, expanding the scope of the structural motifs that can create these organized assemblies is important for the creation of new functional materials.

As part of our ongoing interest in ordered luminescent materials, we report herein liquid crystalline ortho-platinated aryl-pyridyl biscyclometalated complexes. In prior work, our group demonstrated that the core platinum(II) complexes with thienyl

pyridine ligands exhibited strong solid-state and solution luminescent sensory responses to highly toxic cyanogen halides.[17] Square planar non-calamitic metallomesogens adorned with multiple aliphatic sidechains are well known to display columnar phases.[18] Although the one-dimensional columnar structure is attractive, we have been interested in creating lamellar (smectic) phases, which promote robust two-dimensional interconnectivity between molecules. An additional attractive aspect of smectic liquid crystals is that they are generally easier to align than columnar phases and hence these two-dimensional nature would appear to be a better choice for creating charge-transporting and polarized electroluminescent devices. In designing board-like or sandic mesogens[19] rather than more typical calamitic structures we hoped to create superior intermolecular interactions within the smectic layers. We also note that there are limited examples of smectic phases based on sandic molecules.[10,27,28]

The present study describes our investigation of a series of homoleptic ortho-platinated thienyl pyridyl complexes that are functionalized with alkyl chains of varying lengths and we also examine an alternate regioisomer. The mesophases of the molecules, when cooled from the melt, form ordered luminescent solutions.

The homoleptic Pt(II) complexes were prepared by lithiation of the ligands **thpyR (R = $C_{12}H_{25}$, $C_{10}H_{21}$, C_8H_{17}, or C_6H_{13})** with *tert*-BuLi or *n*-BuLi in a THF/Et_2O mixture, followed by metalation with *trans*-$PtCl_2(SEt_2)_2$, according to the procedures of von Zelewsky and coworkers (Scheme 1).[20] The corresponding ligands were prepared *via* a Sonogashira cross-coupling from common dibromide intermediates as described in the electronic supplementary information (ESI). These two intermediates allowed for the facile cross-coupling with alkylalkynes of varying lengths, which are readily hydrogenated to produce alkyl sidechains. The final complexes were chromatographed

under ambient conditions on silica gel and isolated as single stereoisomers, which are

cis in agreement with literature precedent as confirmed by single crystal X-ray

structures (Figure 1, S24–26).[17] All the compounds were characterized by ^{1}H and [13]C

NMR and elemental analysis.
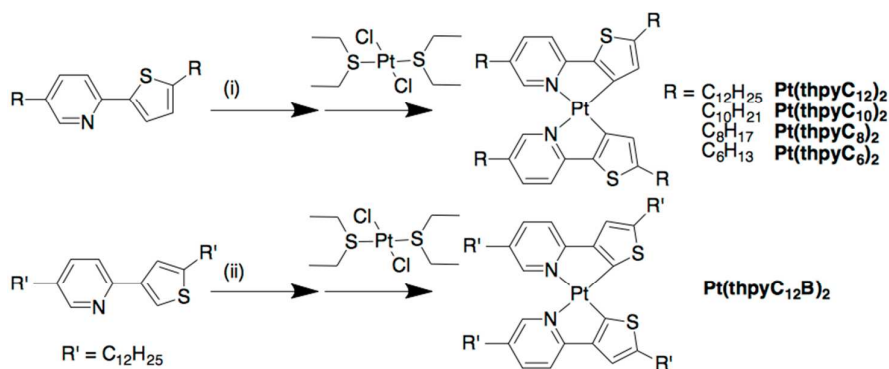
Scheme 1. (i) *t*-BuLi, −78 $^{\circ}$C – 0 $^{\circ}$C, Et$_2$O/THF (ii) *n*-BuLi, −78 °C – 0 °C, Et$_2$O/THF
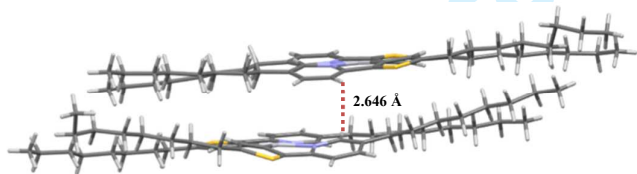

Figure 1. **Pt(thpyC$_8$)$_2$** crystal structure and dimer formation

2. Results and Discussion

We obtained X-ray quality single crystals of **Pt(thpyC$_{12}$B)$_2$** and **Pt(thpyC$_6$)$_2$** with a

space group of $P2_1/c$ and **Pt(thpyC$_8$)$_2$** with a space group of $P2_1$ (Figure 1). We found

that the **Pt(thpyC$_8$)$_2$** complex crystallizes in a dimer structure with the closest

intermolecular association between two aromatic protons of the pyridyl ligands of the

neighboring complexes (2.646 Å, Figure 1). In contrast, the complex with –C$_6$H$_{13}$

chains contain longer intermolecular associations (>3 Å). In previous work, we found

that the non-alkylated complexes showed comparatively shorter distances between the

platinum centers.[17]

To further probe these trends, we investigated the luminescent properties of these homoleptic series and found them to be highly emissive with lifetimes similar to their parent complex.[17,21] The **Pt(thpyC$_n$)$_2$** compounds exhibited very similar photophysical properties and the regioisomer **Pt(thpyC$_{12}$B)$_2$** is blue shifted. This confirms that the luminescence is not dependent on chain length, but on the direct ligand environment.[22] The thin film luminescence decreased in intensity with temperature (the quantum yield, Φ_p, and lifetime, $\tau_p/\mu s$, were determined at 77 K), and the complexes are only weakly emissive in the thin films (Figure S29). The excited state properties of the complexes are understood to have its origin that is comprised of an admixture of [3]ILCT and [3]MLCT character.

Table 1. Photophysical characterization of **Pt(thpyR)$_2$** complexes

Complex	Absorbance λ_{max}/nm (rt)	Emission λ_{max}/nm		Φ_p	$\tau_p/\mu s$
		rt	77 K		
Pt(thpyC$_{12}$)$_2$	435	606	571	0.30	4.5
Pt(thpyC$_{10}$)$_2$	435	605	569	0.28	4.4
Pt(thpyC$_8$)$_2$	435	604	570	0.30	4.6
Pt(thpyC$_6$)$_2$	435	605	571	0.29	4.5
Pt(thpyC$_{12}$B)$_2$	443	585	572	0.28	4.4

We probed phase behavior via differential scanning calorimetry (DSC) and observed several phase transitions suggestive of crystal and liquid crystal phases (Figure 2a, S11–15). Polarized optical microscopy (POM) confirmed this behavior (Figure S17–20).
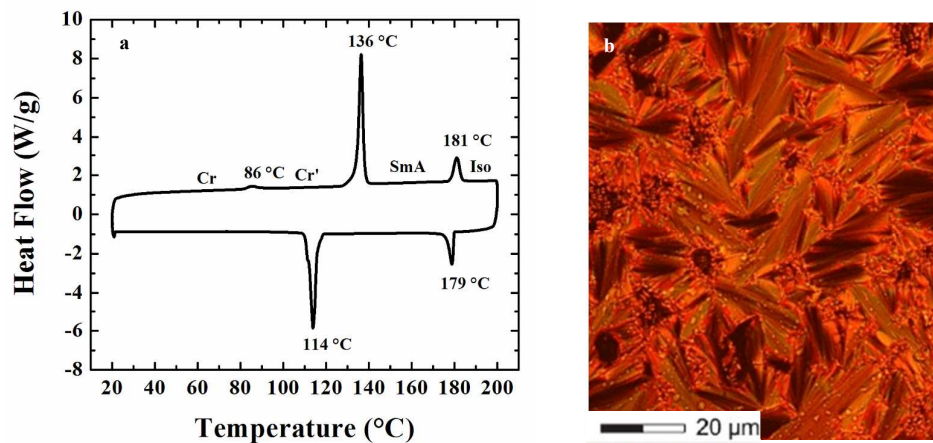

Figure 2. (a) DSC trace from second cycle and (b) POM image at 160 °C of **Pt(thpyC$_8$)$_2$**.

As a representative example, **Pt(thpyC$_8$)$_2$** displayed two low temperature low enthalpy endotherms, suggestive of transitions between minority crystal polymorphs (Figure 2a). The larger enthalpy melting peak at 136 °C gave rise to a smectic A phase. Cooling from the isotropic mixture nucleates as *battonets* and produces a typical SmA texture (Figure 2b). Homeotropic alignment was also observed below the melting transition on hydrophobic slides treated with hexamethyldisilazane (HMDS) (Figure S31). Characteristic SmA textures and similar melting behavior were observed for all compounds we investigated except for **Pt(thpyC$_6$)$_2$**. In addition, a Smectic A to columnar phase sequence is both observed for **Pt(thpyC$_{12}$)$_2$** (Figure S33).

To further characterize the liquid crystalline behavior, we conducted variable temperature X-ray diffraction studies on compounds **Pt(thpyC$_8$)$_2$** and **Pt(thpyC$_{12}$)$_2$**. We observed narrow small-angle and broad wide-angle peaks with little variance over the

temperature range displaying SmA textures (Figure 3, S21–23). As a representative example, **Pt(thpyC$_8$)$_2$**, exhibited a small angle peak of 25 Å, which is similar to the distances between adjacent platinum centers in neighboring lamellae in the crystal structure (Figure 1). The observation of weak (002) and (003) peaks indicate that the layer structure is highly regular. The broad peak at 4.5 – 4.6 Å represents the alkyl tails, while the peak at 3.9 – 4.0 Å represents the core-core distance in the layer.
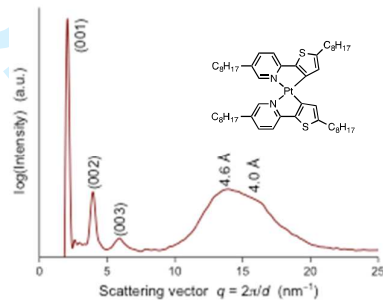
Figure 1. Characteristic smectic A diffraction pattern of **Pt(thpyC$_8$)$_2$** at 160 °C

The trends in the liquid crystal behavior are summarized in Table 2. The mesogenic 2-thienyl substituted complexes were enantiotropic, while in contrast the **Pt(thpyC$_{12}$B)$_2$** exhibited a monotropic Smectic A. **Pt(thpyC$_6$)$_2$** did not display liquid crystalline behavior and melted to give an isotropic liquid. The melting temperature is relatively similar for **Pt(thpyC$_8$)$_2$**, – **Pt(thpyC$_{10}$)$_2$** and **Pt(thpyC$_{12}$)$_2$** compounds, while the clearing temperature increases with decreasing sidechains.

Table 2. Phase transitions and corresponding enthalpy values for the **Pt(thpyR)$_2$** series

Compound	Phase	T(°C)(ΔH(kJ/mol))			Phase
Pt(thpyC$_{12}$)$_2$	Cr	102 (25.0) / 47* → Col$_h$	128 (43.0) / 114 (38.2) → SmA	153 (5.0) / 151 (6.3) →	I
Pt(thpyC$_{10}$)$_2$	Cr	96 (19.2) / 33* → Cr'	129 (36.1) / 105 (31.1) → SmA	164 (6.0) / 160 (6.3) →	I
Pt(thpyC$_8$)$_2$	Cr	86 (0.8) / 114 (27.5) → Cr'	136 (31.6) → SmA	181 (6.7) / 179 (6.5) →	I
Pt(thpyC$_6$)$_2$	Cr		149 (26.3) / 122 (24.4) →		I
Pt(thpyC$_{12}$B)$_2$	Cr		116 (23.9) / 98 (15.8) → SmA ← 111 (4.1)		I

[a]Phase nomenclature. **Cr and Cr'** = crystal structures, **Col$_h$** = hexagonal columnar mesophase, **SmA** = smectic A mesophase, and **I** = isotropic liquid.
[b]Scan rate for all runs was 10 °C/min and phase transitions represent peak maxima and second/third runs.
*Corresponds to a kinetic trapping of crystalline phase

3. Conclusions

In summary, we have designed luminescent Pt(II) square planar complexes that form sandic mesogens, displaying SmA liquid crystal phases. The temperature range of the liquid crystalline phase is dependent upon the alkyl chain length and can be stable over 65 °C. Accessing smectic A phases from sandic square planar cores has attractive prospects for the formation of semiconductive and electrooptical materials.

4. Acknowledgements

5. References

[1] Tschierske C. Development of structural complexity by liquid-crystal self-assembly. Angew Chem Int Ed Engl. 2013;52:8828–8878. DOI: 10.1002/anie.201300872

[2] Lehn J-M. Perspectives in Chemistry–Steps towards Complex Matter. Angew Chem Int Ed Engl. 2013;52:2836–2850. DOI: 10.1002/anie.201208397

[3] Decher G. Fuzzy Nanoassemblies: Toward Layered Polymeric Multicomposites. Science. 1997;277:1232–1237. DOI: 10.1226/science.277.5530.1232

[4] Wong W, He Z, So S, Tong K, Lin Z. A Multifunctional Platinum-Based Triplet Emitter for OLED Applications. Organometallics. 2005;4079–4082. DOI: 10.1021/om050343b

[5] Baldo M, Thompson M, Forrest S. High-efficiency fluorescent organic light-emitting devices using a phosphorescent sensitizer. Nature. 2000;403:750–753. DOI: 10.1038/35001541

[6] Schmidt-Mende L, Fechtenkötter A, Müllen K, Moons E, Friend RH, MacKenzie JD. Self-organized discotic liquid crystals for high-efficiency organic photovoltaics. Science. 2001;293:1119–1122. DOI: 10.1126/science.293.5532.1119

[7] Zhao Q, Li F, Huang C. Phosphorescent chemosensors based on heavy-metal complexes. Chem Soc Rev. 2010;39:3007–3030. DOI: 10.1039/B915340C

[8] Yang X, Huang Z, Dang J, Ho C-L, Zhou G, Wong W-Y. Effective phosphorescence quenching in borylated Pt(II) ppy-type phosphors and their application as I- ion sensors in aqueous medium. Chem Commun. 2013;49:4406–4408. DOI: 10.1039/C2CC37135A

[9] Díez Á, Cowling SJ, Bruce DW. Polarised phosphorescent emission in an organoplatinum(II)-based liquid-crystalline polymer. Chem. Commun. 2012;48:10298–10300. DOI: 10.1039/C2CC35085H

[10] Sato T, Awano H, Katagiri H, Pu Y-J, Takahashi T, Yonetake K. Orientation and Polarized Optical Emission Properties of Platinum(II) Complexes in Smectic Liquid Crystals. Eur J Inorg Chem. 2013;2013:2212–2219. DOI: 10.1002/ejic.201201388

[11] (a) O'Neill M, Kelly SM. Ordered materials for organic electronics and photonics. Adv Mater. 2011;23:566–584. DOI: 10.1002/adma.201002884 (b) Yam VW-W, Wong KM-C, Zhu N. Solvent-Induced Aggregation through Metal×××Metal/π×××π Interactions: Large Solvatochromism of Luminescent Organoplatinum(II) Terpyridyl Complexes. J Am Chem Soc. 2002;124:6506–6507. DOI: 10.1021/ja025811c

[12] Espinet P, Esteruelas M, Oro L. Transition metal liquid crystals: advanced materials within the reach of the coordination chemist. Coord Chem Rev. 1992;215–274. DOI: 10.1016/0010-8545(92)80025-M

[13] Fleischmann E-K, Zentel R. Liquid-crystalline ordering as a concept in materials science: from semiconductors to stimuli-responsive devices. Angew Chem Int Ed Engl. 2013;52:8810–8827. DOI: 10.1002/anie.201300371

[14] Nelson J. Solar energy. Solar cells by self-assembly? Science. 2001;293:1059–1060. DOI: 10.1126/science.1062989

[15] Craats A Van de. Record Charge Carrier Mobility in a Room-Temperature Discotic Liquid-Crystalline Derivative of Hexabenzocoronene. Adv Mater. 1999;1469–1472. DOI: 10.1002/(SICI)1521-4095(199912)11:17<1469::AID-ADMA1469>3.0.CO;2-K

[16] Xiao S, Myers M, Miao Q, Sanaur S, Pang K, Steigerwald ML, Nuckolls C. Molecular wires from contorted aromatic compounds. Angew Chem Int Ed Engl. 2005;44:7390–7394. DOI: 10.1002/anie.200502142 (b) Lamansky S, Kwong RC, Nugent M, Djurovich PI, Thompson ME. Molecularly doped polymer light emitting diodes utilizing phosphorescent Pt(II) and Ir(III) dopants. Organic Electronics. 2001;2:53–62. DOI: 10.1016/S1566-1199(01)00007-6 (c) Krikorian M, Liu S, Swager TM. Columnar Liquid Crystallinity and Mechanochromism in Cationic Platinum(II) Complexes. J Am Chem Soc. 201;136:2952–2955. DOI: 10.1021/ja4114352 (d) Han A, Du P, Sun Z, Wu H, Jia H, Zhang R, Liang Z, Cao R, Eisenberg R. Reversible Mechanochromic Luminescence at Room Temperature in Cationic Platinum(II) Terpyridyl Complexes. Inorg Chem. 2014;53:3338–3344. DOI: 10.1021/ic402624u (e) Ni J, Zhang X, Qiu N, Wu YH, Zhang LY, Zhang J, Chen Z N. Mechanochromic Luminescence Switch of Platinum(II) Complexes with 5-Trimethylsilylethynyl-2,2 '-bipyridine. Inorg Chem. 2011;50:9090–9096. DOI: 10.1021/ic2012777

[17] Thomas SW, Venkatesan K, Müller P, Swager TM. Dark-field oxidative addition-based chemosensing: new bis-cyclometalated Pt(II) complexes and phosphorescent detection of cyanogen halides. J Am Chem Soc. 2006;128:16641–16648. DOI: 10.1021/ja065645z

[18] Laschat S, Baro A, Steinke N, Giesselmann F, Hägele C, Scalia G, Judele R, Kapatsina E, Sauer S, Schreivogel A, Tosoni M. Discotic liquid crystals: from tailor-made synthesis to plastic electronics. Angew Chem Int Ed Engl. 2007;46:4832–4887. DOI: 10.1002/anie.200604203

[19] Herrmann-Schönherr O, Wendorff JH, Ringsdorf H, Tschirner P. Structure of an Aromatic Polyamide with Disk-Like Mesogens in the Main Chain. Makromol Chem Rapid Commun. 1986;7:791–796. DOI: 10.1002/marc.1986.030071207

[20] Chassot L, Mueller E, von Zelewsky A. Cyclometalated Complexes of Platinum(II): Homoleptic Compounds with Aromatic C,N Ligands. Inorg Chem. 1984;4249–4253. DOI: 10.1021/ic00264a018

[21] (a) Maestri M, Sandrini D, Balzani V, Chassot L, Jolliet P, Zelewsky A von. Luminescence of ortho-metallated platinum(II) complexes. Chem Phys Lett. 1985;122:375–379. DOI: 10.1016/0009-2614(85)80240-2 (b) Santoro A, Whitwood AC, Williams JAG, Kozhevnikov VN, Bruce DW. Synthesis, Mesomorphism, and Luminescent Properties of Calamitic 2-Phenylpyridines and Their Complexes with Platinum(II). Chem Mater. 2009;21:3871–3882. DOI: 10.1021/cm9012156

[22] Wadas TJ, Wang Q-M, Kim Y-J, Flaschenreim C, Blanton TN, Eisenberg R. Vapochromism and Its Structural Basis in a Luminescent Pt(II) Terpyridine-Nicotinamide Complex. J Am Chem Soc. 2004;126:16481-16849. DOI: 10.1021/ja047955s

Supporting Information for

Smectic A Mesophases from Luminescent Sandic Platinum(II) Mesogens

Markrete Krikorian,[§a] Constantin-Christian A. Voll,[§a] Maryam Yoon,[a] Koushik Venkatesan,*[b] Paul H. J. Kouwer,*[c] and Timothy M. Swager*[a]

[a] Department of Chemistry, Massachusetts Institute of Technology,
77 Massachusetts Avenue, Cambridge, Massachusetts 02139, USA
[b] Department of Chemistry, University of Zürich,
8057 Zürich, Switzerland. Email: venkatesan.koushik@chem.uzh.ch
[c] Institute for Molecules and Materials, Radboud University Nijmegen, 6525 AJ Nijmegen, The Netherlands. Email: p.kouwer@science.ru.nl
*tswager@mit.edu
[§]These authors contributed equally to the manuscript

Contents

General

Synthesis and Characterization

All reactions were performed under an argon atmosphere despite the stability of the product toward air and moisture, using oven-dried glassware and standard Schlenk techniques. Anhydrous CH_2Cl_2 and THF were obtained from a solvent purification system (Innovative Technologies), and stored under argon.

^{1}H and ^{13}C{^{1}H}NMR spectra were recorded on a Varian 500 MHz spectrometer and referenced to the residual proton or carbon resonance of the deuterated solvent. Electrospray ionization (ESI) high-resolution mass spectrometry (HRMS) was measured on a Bruker Daltonics APEXIV 4.7 Tesla Fourier Transform Ion Cyclotron Resonance Mass Spectrometer and the most abundant masses are reported.

Low-temperature diffraction data (φ-and ω-scans) were collected on a Bruker-AXS X8 Kappa Duo diffractometer coupled to a Smart Apex2 CCD detector with Mo Kα radiation ($\lambda = 0.71073$ Å) from an IμS micro-source. Structures were solved by direct methods using SHELXS[1] and refined against F2 on all data by full-matrix least squares with SHELXL-97.[2] following established refinement strategies.[3–6] All non-hydrogen atoms were refined anisotropically. All hydrogen atoms were included in the model at geometrically calculated positions and refined using a riding model. The isotropic displacement parameters of all hydrogen atoms were fixed to 1.2 times the U value of the atoms they are linked to (1.5 times for methyl groups).

Liquid Crystalline Characterization

Optical microscopy was carried out using standard glass microscope slides on a Leica DM RXP Optical Microscope equipped with a Mettler FP82HT hot stage controlled by Linkham TMS 94 Temperature Controller. Differential scanning calorimetry (DSC) experiments were performed on a TA Instruments Q10 DSC and a TA instruments Discovery DSC. Each sample (3 – 5 mg), sealed in aluminum pans, underwent three heating/cooling cycles from 20 °C to 130 – 190 °C with the rate of 10 °C/min.

High temperature powder X-ray diffraction (XRD) data were collected using a Bruker-AXS X8 Kappa Duo diffractometer coupled to a Smart Apex2 CCD detector with Cu Kα radiation ($\lambda = 1.5418$ Å) from an IμS micro-source. Kapton tubing and a single-crystal mounting pin were used to mount the crushed powder samples. XRD data is shown as the intensity as a function of the length of θ and the (layer) spacing d is calculated using $n\lambda = 2d \sin\theta$, Bragg's Law, where θ is the scattering angle, n is an integer and λ is the wavelength. The data workup was performed using the FullProf:WinPlotr program, which allowed for baseline correction and easy interconversion from θ to d.

Photophysical Characterization

UV/Vis spectra were recorded on an Agilent 8453 diode-array spectrophotometer. Emission spectra were acquired on a SPEX Fluorolog fluorometer (model FL-321, 450 W xenon lamp) using right-angle detection (solution measurements). All room temperature solution samples for emission spectra were degassed with Ar in an anaerobic cuvette. Quantum yields of phosphorescence were determined by comparison to Ru(bpy)$_3$ in deoxygenated water and are corrected for solvent refractive index and absorption differences at the excitation wavelength.

Preparation of 5-bromo-2-(5-bromothiophen-2-yl)pyridine

A mixture of 5-bromo-2-iodopyridine (5.77 g, 20.0 mmol) and Pd(PPh₃)₄ in 1,2-dimethoxy ethane (35 mL) was purged with argon for 15 mins. To this solution (5-bromothiophen-2-yl)boronic acid (4.14 g, 20.0 mmol) in ethanol (35 mL) was added and the resulting mixture was stirred for 15 mins with further argon bubbling. The reaction mixture was heated at reflux for 24 h, cooled down and concentrated *in vacuo*. The residue was extracted with CH_2Cl_2, washed with water and saturated brine. The combined organics were dried over $MgSO_4$ and concentrated *in vacuo*. Chromatography on silica gel (2:1 hexanes/CH_2Cl_2) gave 1.8 g of the product (28%).
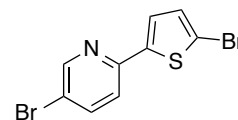
Preparation of 5-dodecyl-2-(5-dodecylthiophen-2-yl)pyridine

A mixture of 5-bromo-2-(5-bromothiophen-2-yl)pyridine (1.80 g, 5.64 mmol), 1-dodecyne (2.99 g, 17.4 mmol), PdCl₂(PPh₃)₂ (0.22 g, 0.31 mmol), CuI and triethylamine (30 mL) was purged with argon for 15 mins. After 30 h of heating at reflux, the reaction mixture was cooled down and the solvent removed by reduced pressure. The residue was extracted with CH_2Cl_2, washed with water and saturated brine. The combined organics were dried over $MgSO_4$, filtered and concentrated *in vacuo*. Chromatography on silica gel (1:2 CH_2Cl_2/hexanes) gave 1.8 g of 5-(dodec-1-yn-1-yl)-2-(5-(dodec-1-yn-1-yl)thiophen-2-yl)pyridine (65%).
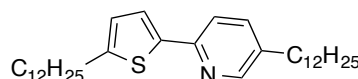
5-(dodec-1-yn-1-yl)-2-(5-(dodec-1-yn-1-yl)thiophen-2-yl)pyridine (2.0 g, 4.0 mmol) and Pd/C (2.0 g) in ethyl acetate (35 mL) was reacted in a parr bomb with H₂ at a pressure of 45 psi for 12 h. The reaction mixture was then filtered over celite. The residue was washed with CH_2Cl_2 and EtOAc and the filtrate was evaporated *in vacuo* to yield an off-white solid. The solid was chromatographed on silica gel using CH_2Cl_2/hexanes (1:1) as the eluent to yield a white solid (1.9 g, 52%).

Preparation of 5-decyl-2-(5-decylthiophen-2-yl)pyridine

A mixture of 5-bromo-2-(5-bromothiophen-2-yl)pyridine (1.0 g, 3.1 mmol), 1-decyne (1.33 g, 9.44 mmol), PdCl₂(PPh₃)₂ (0.109 g, 0.215 mmol), CuI (0.033 g) and triethylamine (30 mL) was subjected to argon bubbling. After 30 h of heating at reflux, the reaction mixture was cooled down and the solvent removed by reduced pressure. The residue was extracted with CH_2Cl_2, washed with water and saturated brine. The combined organics were dried over $MgSO_4$, filtered and concentrated *in vacuo*. Chromatography on silica gel (1:2 CH_2Cl_2/hexane) gave 0.9 g of 5-(dec-1-yn-1-yl)-2-(5-(dec-1-yn-1-yl)thiophen-2-yl)pyridine (91%).
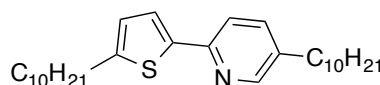
5-(dec-1-yn-1-yl)-2-(5-(dec-1-yn-1-yl)thiophen-2-yl)pyridine (0.88 g, 0.63 mmol) and Pd/C (0.033 g) in ethyl acetate (35 mL) was reacted in a parr bomb with H₂ at a pressure of 45 psi for 12 h. The reaction mixture was then filtered over celite. The residue was washed with CH_2Cl_2 and EtOAc and the filtrate was evaporated *in vacuo* to yield an off-white solid. The solid was chromatographed on silica gel using CH_2Cl_2/hexanes (1:1) as the eluent to yield a white solid (0.33 g, 26%).

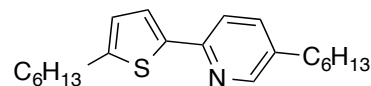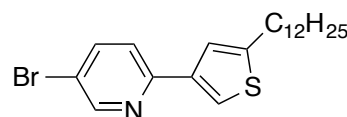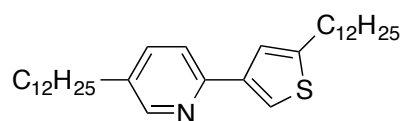**Preparation of 5-octyl-2-(5-octylthiophen-2-yl)pyridine**

A mixture of 5-bromo-2-(5-bromothiophen-2-yl)pyridine (1.0 g, 3.1 mmol), 1-decyne (1.03 g, 7.45 mmol), PdCl₂(PPh₃)₂ (0.11 g, 0.22 mmol), CuI (0.033 mg) and triethylamine (30 mL) was subjected to argon bubbling. After 30 h of heating at reflux, the reaction mixture was cooled down and the solvent removed by reduced pressure. The residue was extracted with CH_2Cl_2, washed with water and saturated brine. The combined organics were dried over $MgSO_4$, filtered and concentrated *in vacuo*. Chromatography on silica gel (1:2 CH_2Cl_2/hexanes) gave 1.1 g of 5-(oct-1-yn-1-yl)-2-(5-(oct-1-yn-1-yl)thiophen-2-yl)pyridine (82%).
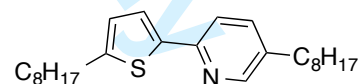
5-(oct-1-yn-1-yl)-2-(5-(oct-1-yn-1-yl)thiophen-2-yl)pyridine (1.1 g, 2.9 mmol) and Pd/C (1.0 g) in ethyl acetate (35 mL) was reacted in a parr bomb with H₂ at a pressure of 45 psi for 12 h. The reaction mixture was then filtered over celite. The residue was washed with CH_2Cl_2 and EtOAc and the filtrate was evaporated *in vacuo* to yield an off-white solid. The solid was chromatographed on silica gel using CH_2Cl_2/hexanes (1:1) as the eluent to yield a white solid (0.6 g, 54%).

Preparation of 5-hexyl-2-(5-hexylthiophen-2-yl)pyridine

A mixture of 5-bromo-2-(5-bromothiophen-2-yl)pyridine (2.0 g, 6.3 mmol), 1-hexyne (2.1 g, 25.0 mmol), $PdCl_2(PPh_3)_2$ (0.22 g, 0.22 mmol), CuI (0.066 g, 0.31 mmol) and triethylamine (30 mL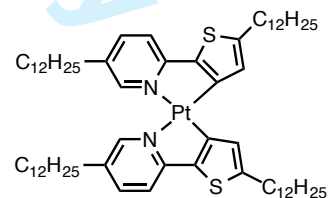) was subjected to argon bubbling. After 30 h of heating at reflux, the reaction mixture was cooled down and the solvent removed by reduced pressure. The residue was extracted with CH_2Cl_2, washed with water and saturated brine. The combined organics were dried over $MgSO_4$, filtered and concentrated *in vacuo*. Chromatography on silica gel (2:1 CH_2Cl_2/hexanes) gave 1.3 g of 5-(hex-1-yn-1-yl)-2-(5-(hex-1-yn-1-yl)thiophen-2-yl)pyridine (65%).

5-(hex-1-yn-1-yl)-2-(5-(hex-1-yn-1-yl)thiophen-2-yl)pyridine (1.3 g, 4.0 mmol) and Pd/C (1.2 g) in ethyl acetate (35 ml) was reacted in a parr bomb with H_2 at a pressure of 45 psi for 12 h. The reaction mixture was then filtered over celite. The residue was washed with CH_2Cl_2 and EtOAc and the filtrate was evaporated *in vacuo* to yield an off-white solid. The solid was chromatographed on silica gel using CH_2Cl_2/hexanes (2:1) as the eluent to yield a white solid (1.1 g, 83%).

Preparation of 5-bromo-2-(5-dodecylthiophen-3-yl)pyridine

A mixture of 5-bromo-2-iodopyridine (1.66 g, 5.53 mmol), $Pd(PPh_3)_4$ (0.32 g, 0.33 mmol) and 2M Na_2CO_3 in 1,2-dimethoxy ethane (100 mL) was purged with argon for 15 min. To this solution (5-dodecylthiophen-3-yl)boronic acid (2.1 g, 7.1 mmol) was added and the resulting mixture was stirred for 15 min with further argon bubbling. The reaction mixture was heated at reflux for 24 h, cooled down and concentrated *in vacuo*. The residue was extracted with CH_2Cl_2, washed with water and saturated brine. The combined organics were dried over $MgSO_4$ and concentrated *in vacuo*. Chromatography on silica gel (1:1 CH_2Cl_2/hexanes) gave 1.3 g of the product (58%).

Preparation of 5-dodecyl-2-(5-dodecylthiophen-3-yl)pyridine

A mixture of 5-bromo-2-(5-dodecylthiophen-3-yl)pyridine (1.4 g, 3.43 mmol), 1-hexyne (1.1 g, 14 mmol), $PdCl_2(PPh_3)_2$ (0.12 mg, 0.10 mmol), CuI (0.032 mg, 0.22 mmol) and triethylamine (30 mL) was subjected to argon bubbling. After 30 h of heating at reflux, the reaction mixture was cooled down and the solvent removed by reduced pressure. The residue was extracted with CH_2Cl_2, washed with water and saturated brine. The combined organics were dried over $MgSO_4$, filtered and concentrated *in vacuo*. Chromatography on silica gel (2:1 CH_2Cl_2/hexanes) gave 1.3 g of 5-(dodec-1-yn-1-yl)-2-(5-dodecylthiophen-3-yl)pyridine (77%).

5-(dodec-1-yn-1-yl)-2-(5-dodecylthiophen-3-yl)pyridine (1.3 g, 2.6 mmol) and Pd/C (1.2 g) in ethyl acetate (100 mL) was reacted in a parr bomb with H_2 at a pressure of 45 psi for 12 h. The reaction mixture was then filtered over celite. The residue was washed with CH_2Cl_2 and EtOAc and the filtrate was evaporated *in vacuo* to yield an off-white solid. The solid was chromatographed on silica gel using CH_2Cl_2/hexanes (2:1) as the eluent to yield a white solid (0.8 g, 60%).

Preparation of Pt(thpyC$_{12}$)$_2$

A solution of *trans*-PtCl$_2$(Et$_2$S)$_2$ (0.34 g, 0.75 mmol) in diethyl ether and THF was added dropwise to a stirred solution of lithiated ligand from 5-dodecyl-2-(5-dodecylthiophen-2-yl)pyridine (1.0 g, 3.0 mmol) and 1.6 M *t*-BuLi (3.6 mL, 6.0 mmol) in ether at −78 °C. After the solution was stirred for 30 min at −78 °C, the temperature was allowed to rise slowly to 0 °C. The reaction mixture was hydrolyzed at 0 °C. The organic phase was washed with saturated brine and the aqueous phase was extracted with CH_2Cl_2. The combined extracts were dried over $MgSO_4$. The organic layer was evaporated to yield a red oily residue. The residue was chromatographed on silica gel with CH_2Cl_2/hexanes (1:2) as the eluent to give 0.14 g (21%) of **Pt(thpyC$_{12}$)$_2$** as an orange solid.

Anal. Calcd. for $C_{66}H_{108}N_2PtS_2$: C, 66.68; H, 9.16; N, 2.36. Found: *C, 66.41; H, 9.08; N, 2.18*.

1
2
3
4
5
6
7
8
9
10

^{1}H-NMR (500 MHz, CDCl$_3$): δ 8.40 (1H, s), 7.53 (1H, dd, J = 8.1, 1.2), 7.32 (1H, s), 7.28 (1H, d, J = 8.1), 2.93 (2H, t, J = 7.5), 2.62 (2H, t, J = 7.5), 1.74 (2H, quin, J = 7.4), 1.65 (2H, quin, J = 7.0), 1.52 – 1.20 (40H, b), 0.91 – 0.85 (6H, b).
^{13}C-NMR (126 MHz, CDCl$_3$): δ 160.4, 149.6, 148.3, 148.0, 140.6, 139.2, 134.0, 117.6, 33.7, 32.6, 32.6, 32.6, 32.0, 31.4, 30.4, 30.4, 30.4, 30.4, 30.4, 30.3, 30.3, 30.2, 30.2, 30.1, 30.0, 30.0, 29.9, 29.9, 23.4, 23.4, 23.4, 14.8, 14.8.
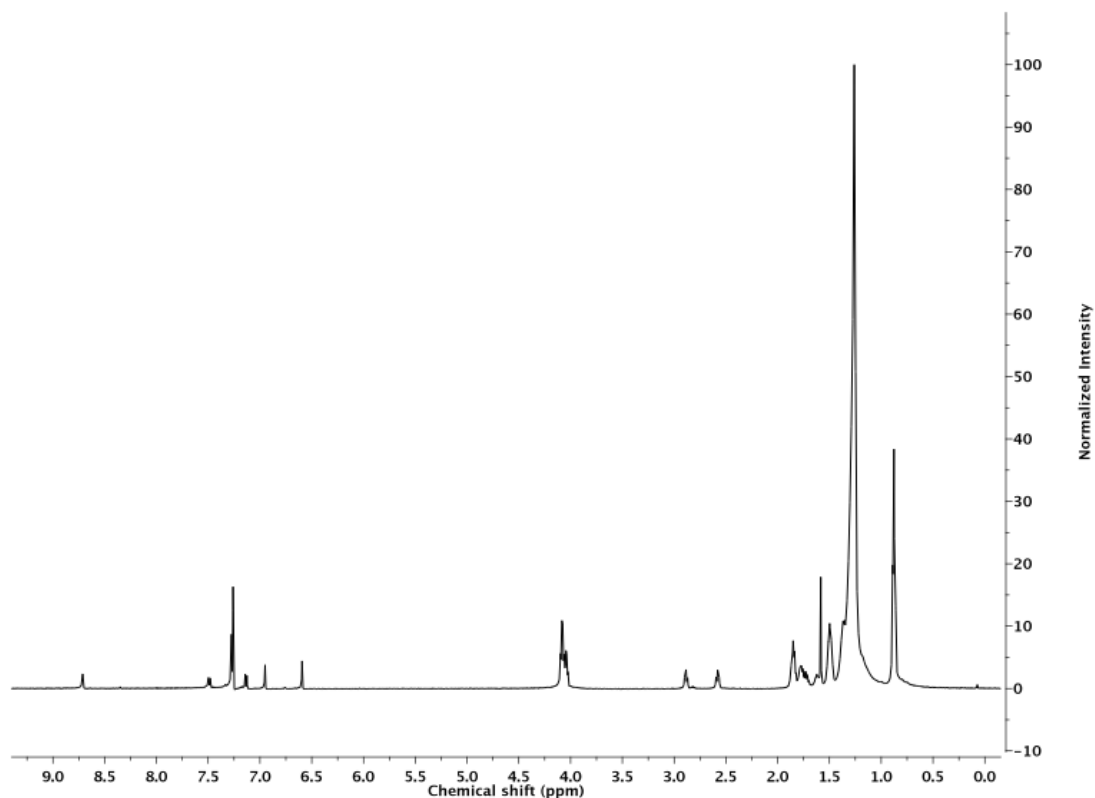
Figure S1: ^{1}H NMR of **Pt(thpyC$_{12}$)$_2$**
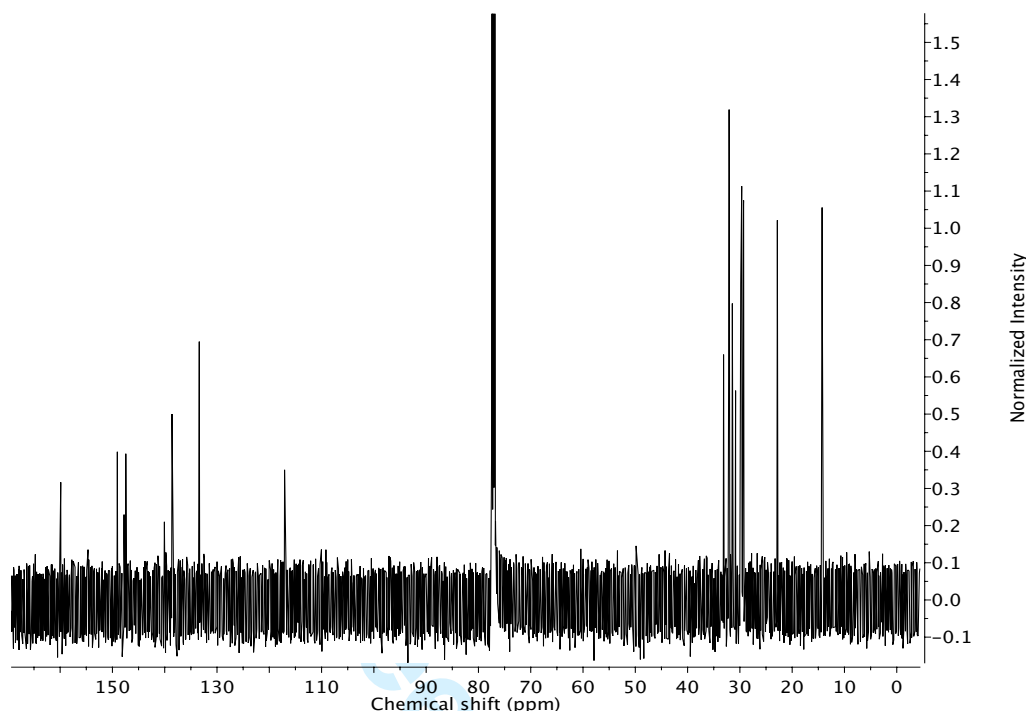
Figure S2: ^{13}C NMR of **Pt(thpyC$_{12}$)$_2$**

Preparation of Pt(thpyC$_{12}$B)$_2$ the other isomer

trans-PtCl$_2$(Et$_2$S)$_2$ (0.5 g, 1.1 mmol) in diethyl ether and THF (4:1) at -78 °C was added dropwise to a stirred solution of lithiated ligand from 5-dodecyl-2-(5-dodecylthiophen-2-yl)pyridine (0.6 g, 1.3 mmol) and 1.6 M *t*-BuLi (0.8 mL, 1 mmol) stirred at −78 °C for 1 h. The mixture was reacted for 30 min before the temperature was raised to 0 °C and allowed to stir for another 30 min. Ethanol was added and the organic layer was separated and extracted with CH$_2$Cl$_2$. The combined organic phases were dried over Na$_2$SO$_4$, filtered and dried *in vacuo*. Chromatography on silica gel (1:3 CH$_2$Cl$_2$/hexanes) gave 0.2 g (44%) of **Pt(thpyC$_{12}$B)$_2$** as a brown solid.
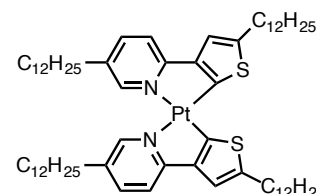
Anal. Calcd for C$_{66}$H$_{108}$N$_2$PtS$_2$: C, 66.68; H, 9.16; N, 2.36. Found: *C, 66.40; H, 9.24; N, 2.11*.

^{1}H-NMR (500 MHz, CDCl$_3$): δ 8.39 (1H, s), 7.53 (1H, d, *J* = 8.1), 7.29 (1H, d, *J* = 8.1), 6.91 (1H, s), 2.82 (2H, t, *J* = 7.6), 2.59 (2H, t, *J* = 7.6), 1.73 (2H, quin, *J* = 7.5), 1.64 (2H, quin, *J* = 7.6), 1.4 – 1.2 (30H, m), 0.9 (6H, m).
^{13}C-NMR (126 MHz, CDCl$_3$): δ 159.8, 149.0, 147.8, 147.4, 140.1, 138.6, 133.4, 117.1, 33.1, 32.1, 32.1, 31.4, 30.8, 29.8, 29.8, 29.8, 29.7, 29.7, 29.5, 29.5, 29.3, 29.3, 22.9, 22.8, 14.3, 14.3.

1
2
3
4
5
6
7
8
9
10
11
12
13
14
15
16
17
18
19
20
21
22
23
24
25
26
27
28
29
30
31
32
33
34
35
36
37
38
39
40
41
42
43
44
45
46
47
48
49
50
51
52
53
54
55
56
57
58
59
60
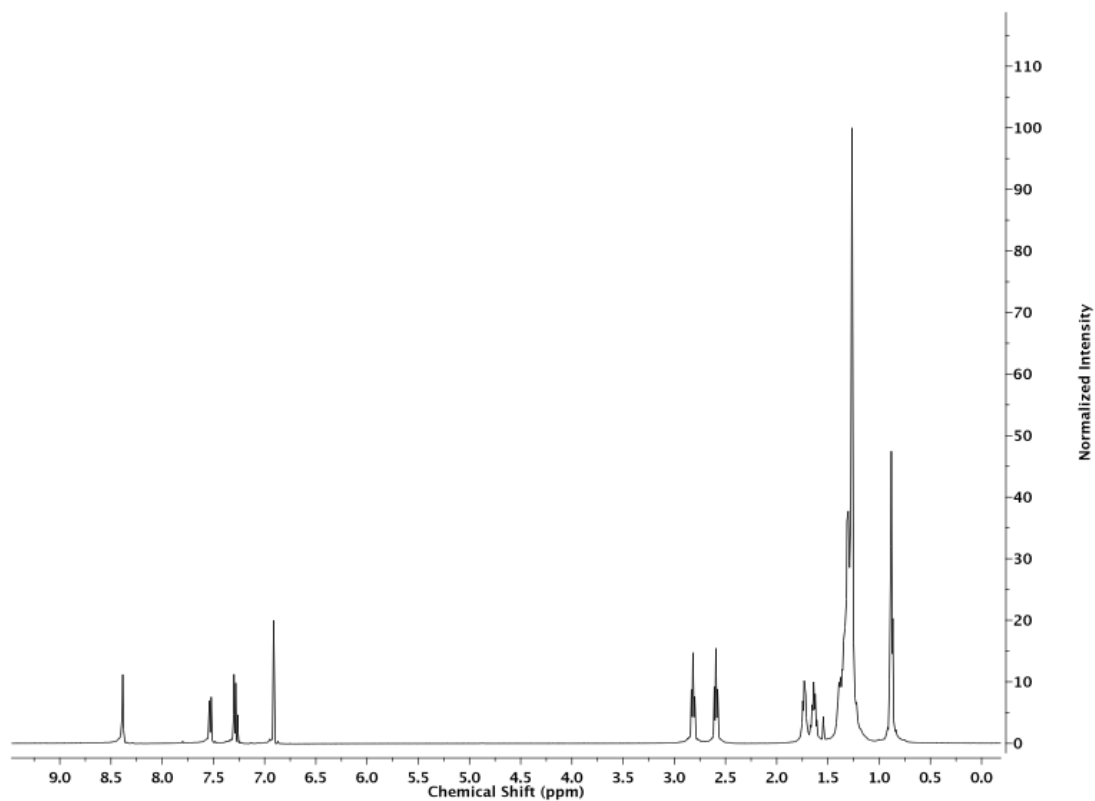
Figure S3: ^{1}H NMR of **Pt(thpyC$_{12}$B)$_2$**
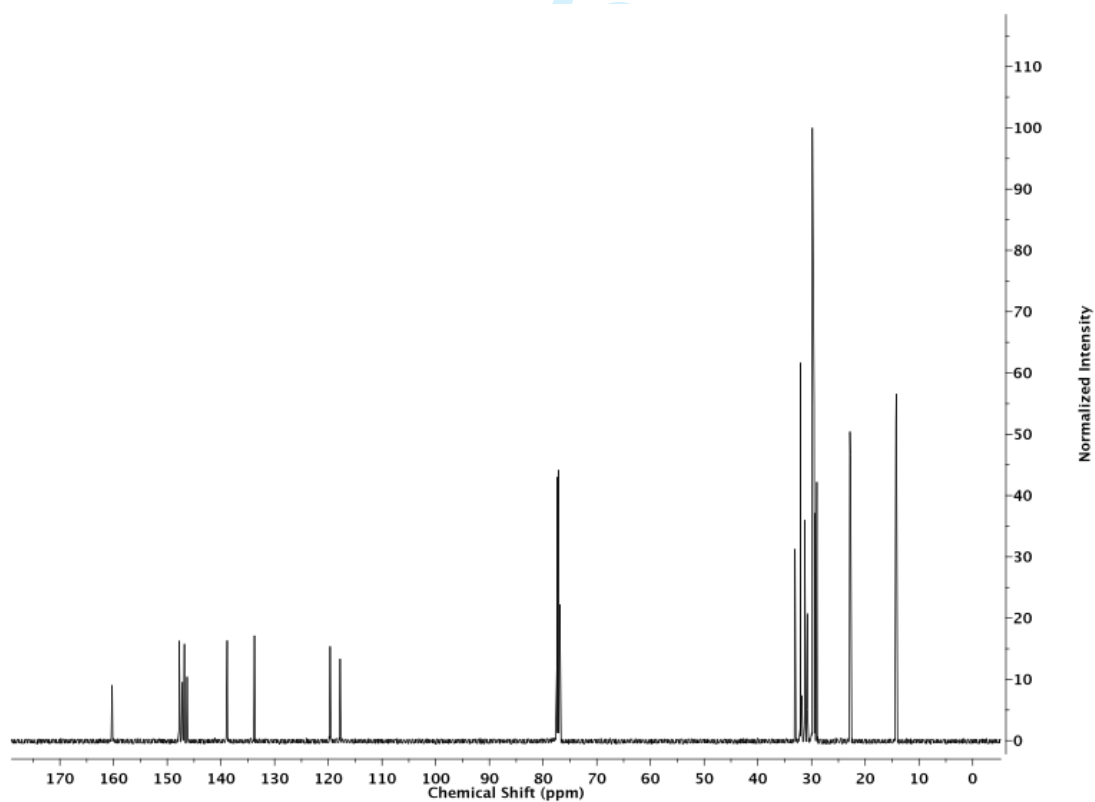
Figure S4: ^{13}C NMR of **Pt(thpyC$_{12}$B)$_2$**

S6

Preparation of Pt(thpyC$_{10}$)$_2$

trans-PtCl$_2$(Et$_2$S)$_2$ (0.5 g, 1 mmol) in diethyl ether and THF was added dropwise to a stirred solution of lithiated ligand from 5-decyl-2-(5-decylthiophen-2-yl)pyridine (0.9 g, 6 mmol) and 1.6 M *t*-BuLi (6.6 mL, 11 mmol) at −78 °C. Chromatography on silica gel (2:1 CH$_2$Cl$_2$/hexanes) gave 0.6 g of an orange solid, **Pt(thpyC$_{10}$)$_2$** in 51% yield.
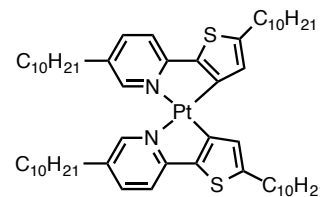
Anal. Calcd. for C$_{58}$H$_{92}$N$_2$PtS$_2$: C, 64.71; H, 8.61; N, 2.60. Found: *C, 64.79; H, 8.76; N, 2.30.*

^{1}H-NMR (500 MHz, CDCl$_3$): δ 8.40 (1H, s), 7.53 (1H, dd, *J* = 8.2, 1.7), 7.32 (1H, s), 7.27 (1H, d, *J* = 8.2), 2.93 (2H, t, *J* = 7.5), 2.61 (2H, t, *J* = 7.5), 1.74 (2H, quin, *J* = 7.4), 1.65 (2H, quin, *J* = 7.4), 1.42 (2H, m), 1.37 – 1.20 (28H, m), 0.87 (3H, t, *J* = 6.9), 0.87 (3H, t, *J* = 6.9).
^{13}C-NMR (126 MHz, CDCl$_3$): δ 159.8, 149.0, 147.8, 147.4, 140.1, 138.6, 133.4, 117.1, 33.1, 32.1, 32.1, 31.4, 30.8, 29.8, 29.8, 29.8, 29.7, 29.7, 29.5, 29.5, 29.3, 29.3, 22.9, 22.8, 14.3, 14.3.
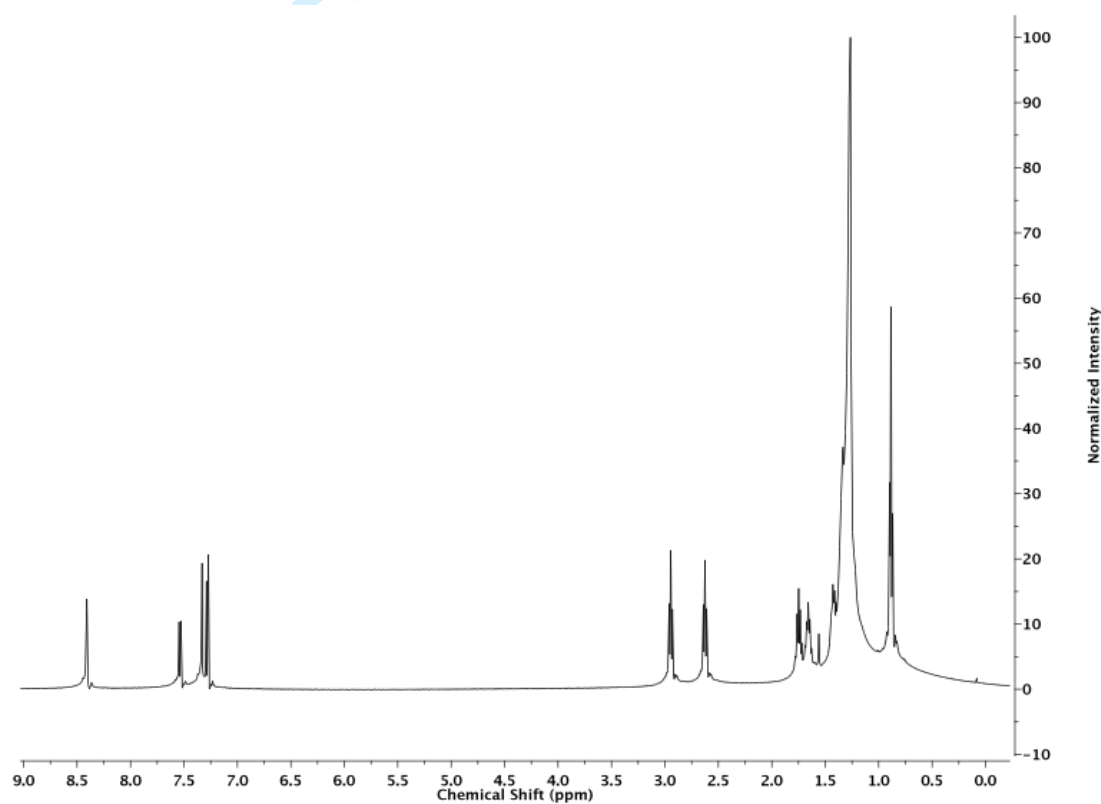
Figure S5: ^{1}H NMR of **Pt(thpyC$_{10}$)$_2$**
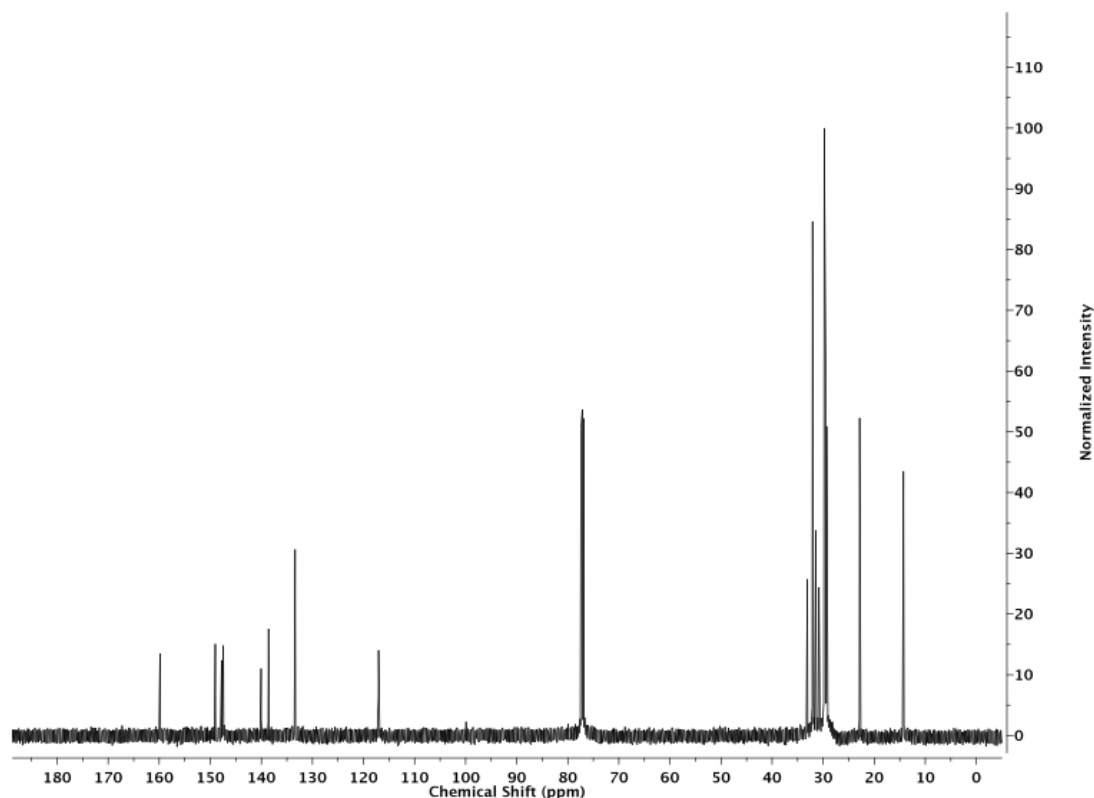
Figure S6: ^{13}C NMR of **Pt(thpyC$_{10}$)$_2$**

Preparation of Pt(thpyC$_8$)$_2$

trans-PtCl$_2$(Et$_2$S)$_2$ (0.50 g, 1.1 mmol) in diethyl ether and THF was added dropwise to a stirred solution of lithiated ligand from 5-octyl-2-(5-octylthiophen-2-yl)pyridine (0.91 g, 5.6 mmol) and 1.6 M t-BuLi (6.6 mL, 11 mmol) at –78 °C. Chromatography on silica gel (2:1 CH$_2$Cl$_2$/hexanes) gave 0.54 g of a dark orange solid, **Pt(thpyC$_8$)$_2$** in 51% yield.
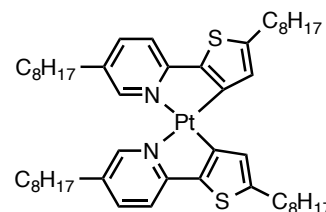
Anal. Calcd. for C$_{50}$H$_{76}$N$_2$PtS$_2$: C, 62.27; H, 7.94; N, 2.90. Found: C, 61.91; H, 7.67; N, 2.74.

^{1}H-NMR (500 MHz, CDCl$_3$): δ 8.39 (1H, s), 7.51 (1H, d, J = 8.2), 7.32 (1H, s), 7.26 (1H, d, J = 8.3), 2.93 (2H, t, J = 7.2), 2.60 (2H, t, J = 7.2), 1.74 (2H, quin, J = 7.2), 1.64 (2H, quin, J = 6.9), 1.42 (2H, quin, J = 6.9), 1.38 – 1.11 (18H, b), 0.93 – 0.82 (6H, b).
^{13}C-NMR (126 MHz, CDCl$_3$): δ 160.4, 149.5, 148.3, 148.0, 140.6, 139.1, 134.0, 133.9, 117.6, 33.7, 32.6, 32.6, 32.0, 31.4, 30.2, 30.2, 30.0, 30.0, 29.9, 29.9, 23.4, 23.4, 14.8, 14.8.
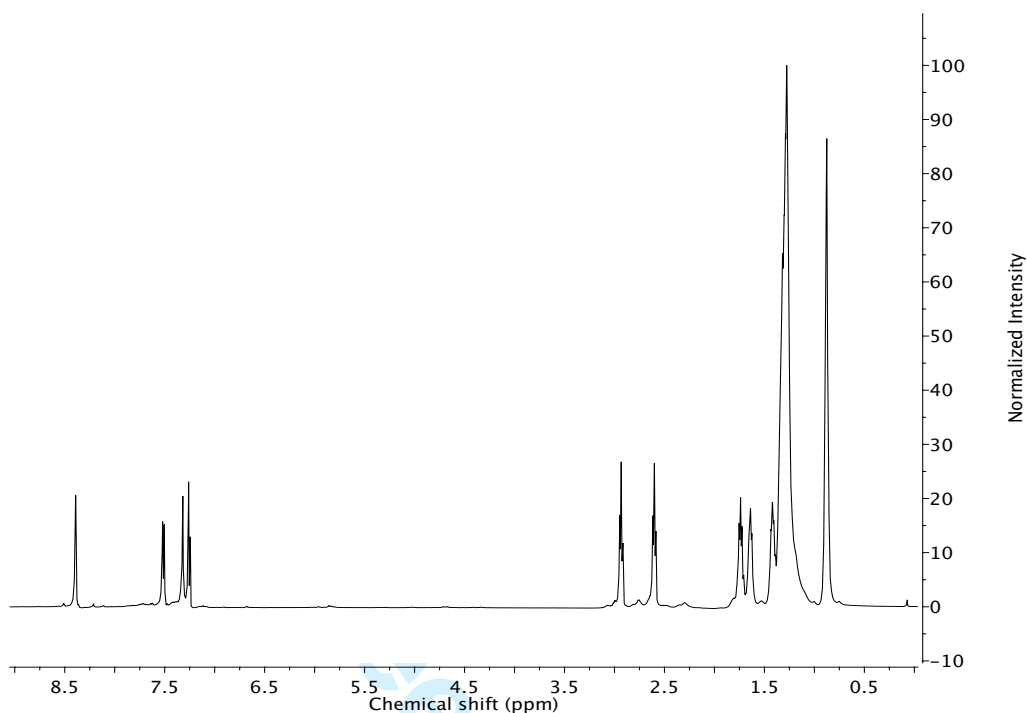
Figure S7: ^{1}H NMR of **Pt(thpyC$_8$)$_2$**
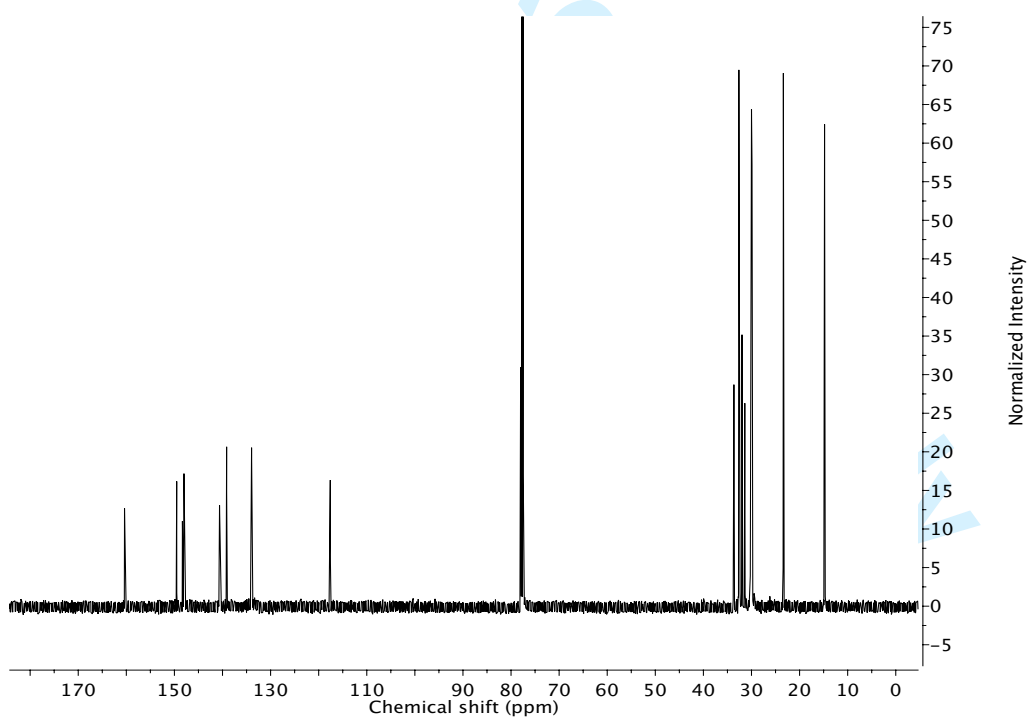
Figure S8: ^{13}C NMR of **Pt(thpyC$_8$)$_2$**

Preparation of Pt(thpyC$_6$)$_2$

A solution of trans-PtCl$_2$(Et$_2$S)$_2$ (0.34 g, 0.75 mmol) in diethyl ether and THF was added dropwise to a stirred solution of
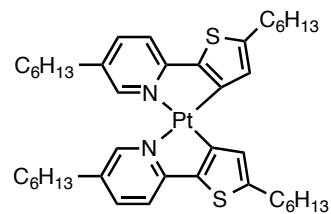
lithiated ligand [from 5-hexyl-2-(5-hexylthiophen-2-yl)pyridine (1.0 g, 3.0 mmol) and 1.6 M *t*-BuLi (3.6 mL, 6.0 mmol) in ether at −78 °C. After the solution was stirred for 30 min, the temperature was allowed to rise slowly to 0 °C. The reaction mixture was hydrolyzed at 0 °C. The organic phase was washed with saturated brine and the aqueous phase extracted with CH_2Cl_2. The combined extracts were dried over $MgSO_4$. The organic layer was evaporated to yield a red oily residue. The residue was chromatographed on silica gel with CH_2Cl_2:hexanes (1:2) as the eluent to give 0.140 g (21%) of **Pt(thpyC$_6$)$_2$** as an orange solid.

Anal. Calcd for $C_{42}H_{60}N_2PtS_2$: C, 59.20; H, 7.10; N, 3.29. Found: *C, 59.01; H, 6.78; N, 3.05*.

^{1}H-NMR (500 MHz, CDCl$_3$): δ 8.39 (1H, s), 7.52 (1H, dd, *J* = 8.2, 1.8), 7.32 (1H, s), 7.26 (1H, *J* = 8.1), 2.94 (2H, t, *J* = 7.5), 2.61 (2H, t, *J* = 7.6), 1.74 (2H, quin, *J* = 7.6), 1.64 (2H, quin, *J* = 7.6), 1.43 (2H, m), 1.4 – 1.2 (12H, m), 0.89 (6H, m).
^{13}C-NMR (126 MHz, CDCl$_3$): δ 159.9, 149.0, 147.8, 147.5, 140.1, 138.6, 133.4, 117.1, 33.1, 32.0, 31.9, 31.8, 31.4, 30.8, 29.0, 29.0, 22.8, 22.7, 14.3, 14.2.
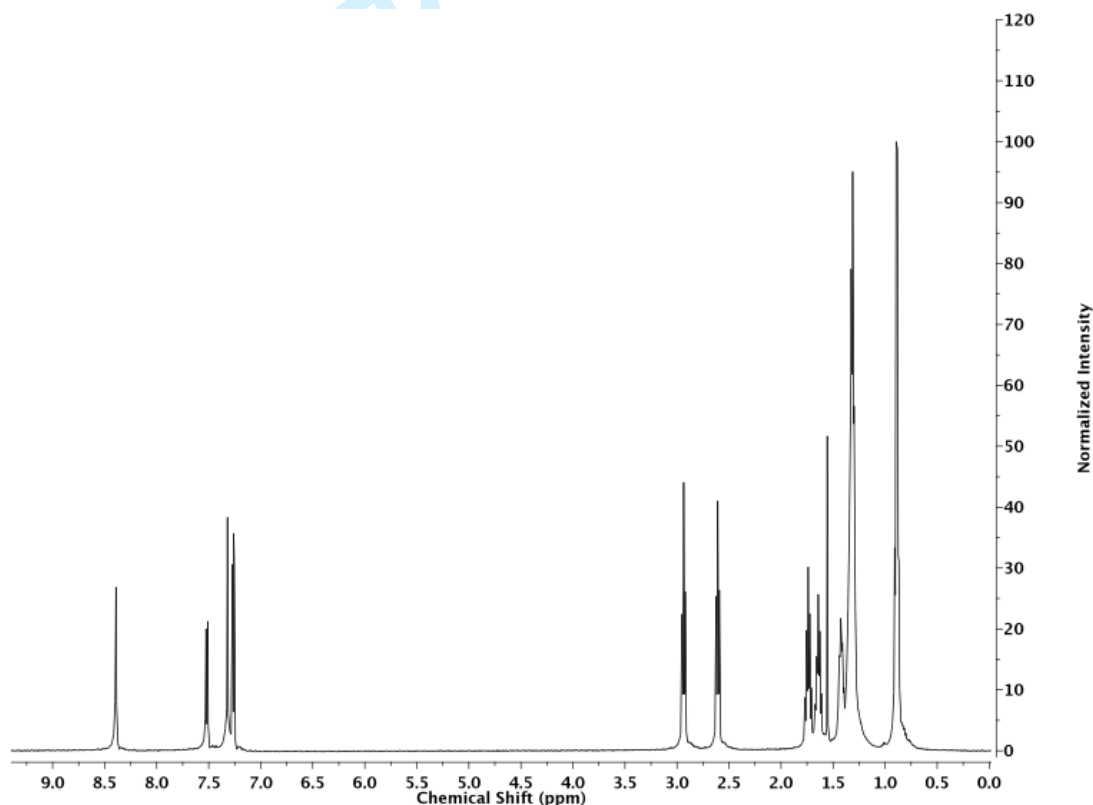
Figure S9: ^{1}H NMR of **Pt(thpyC$_6$)$_2$**
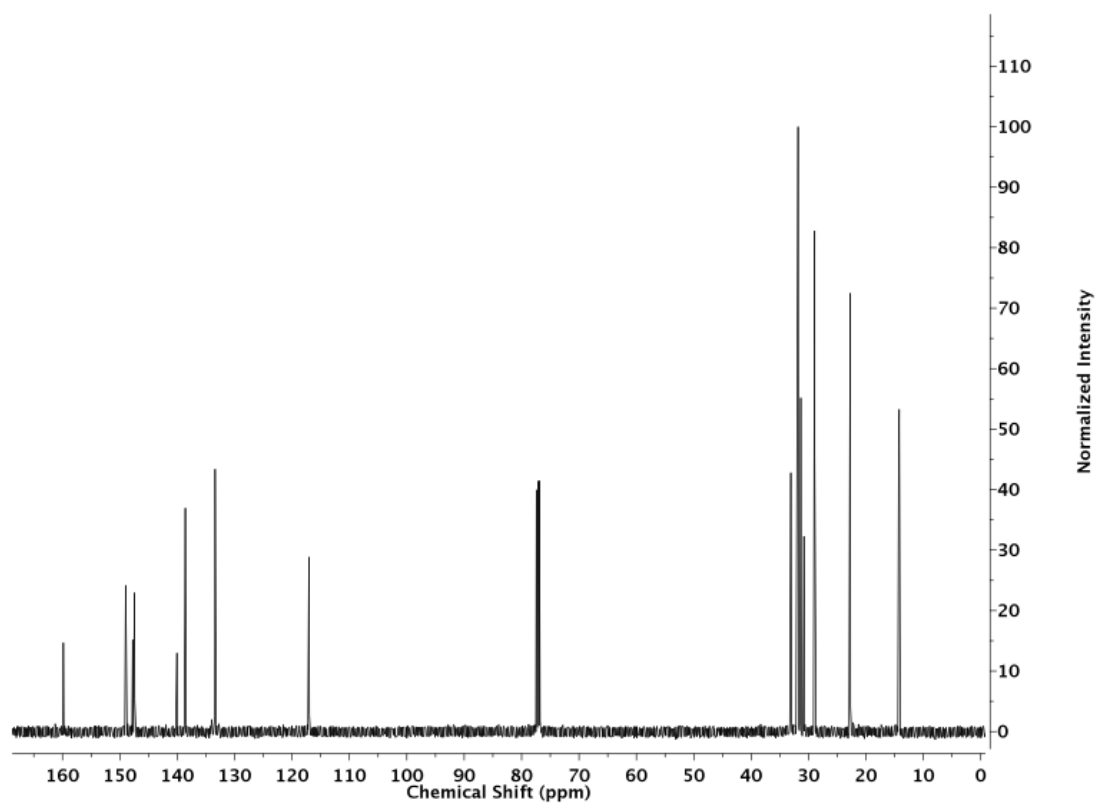
Figure S10: ^{13}C NMR of **Pt(thpyC$_6$)$_2$**

DSC and TGA Data

All DSC were collected using a heating and cooling rate of 10 °C/min.

Figure S11: **Pt(thpyC₁₂)₂** DSC Cycle 1
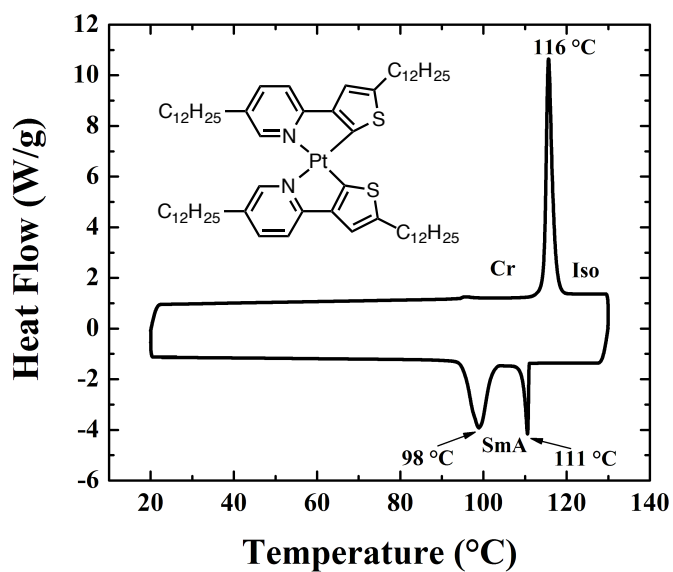
Figure S12: **Pt(thpyC₁₂B)₂** DSC Cycle 2
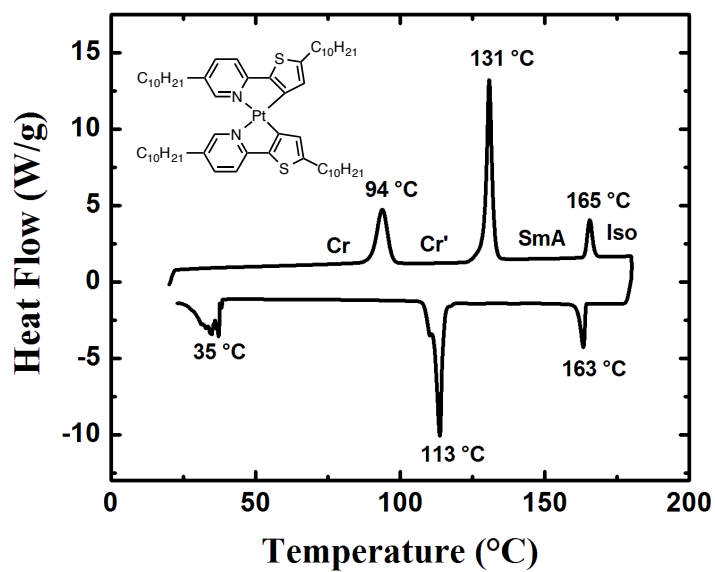
Figure S13: **Pt(thpyC₁₀)₂** DSC Cycle 2
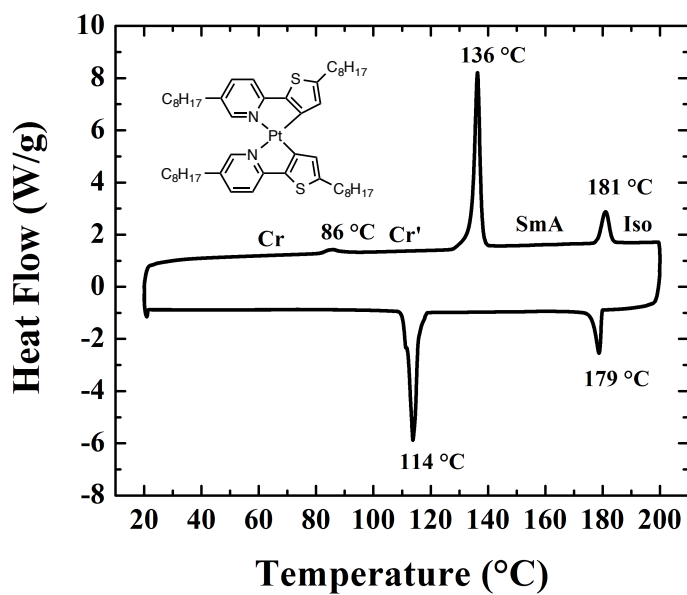
Figure S14: **Pt(thpyC₈)₂** DSC Cycle 2
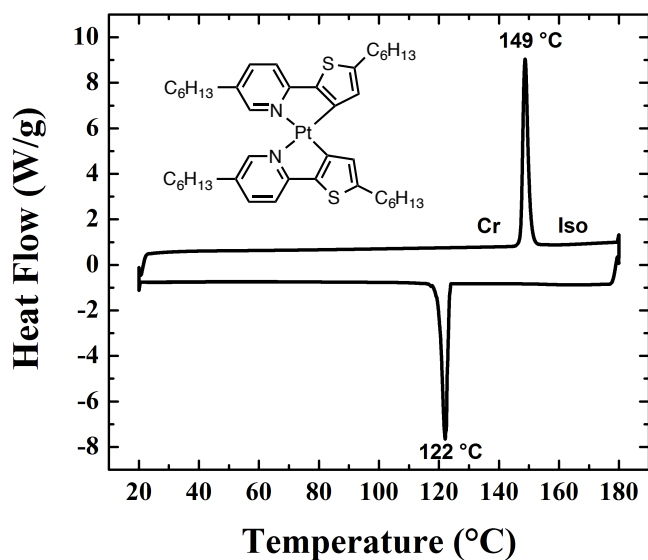
Figure S15: **Pt(thpyC$_6$)$_2$** DSC Cycle 2
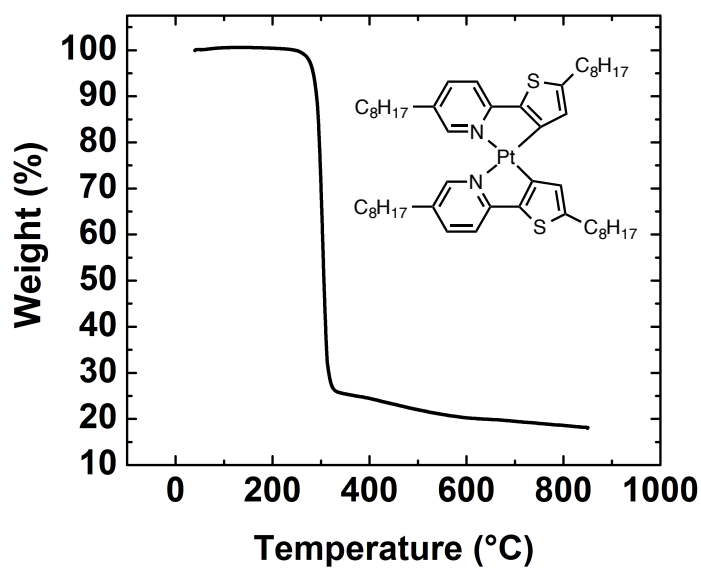
Figure S16: TGA data of **Pt(thpyC$_8$)$_2$**

Polarized Optical Microscope Studies
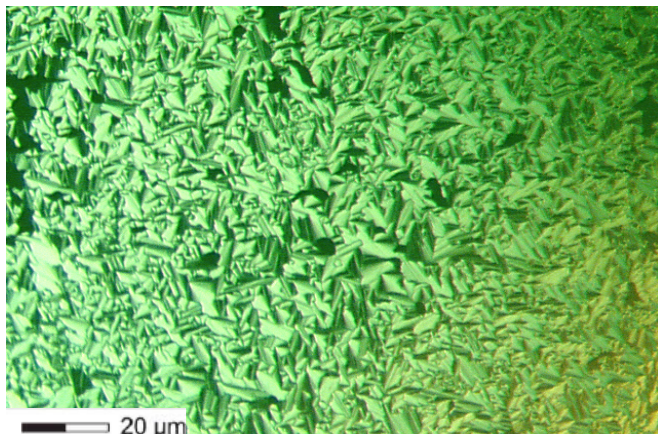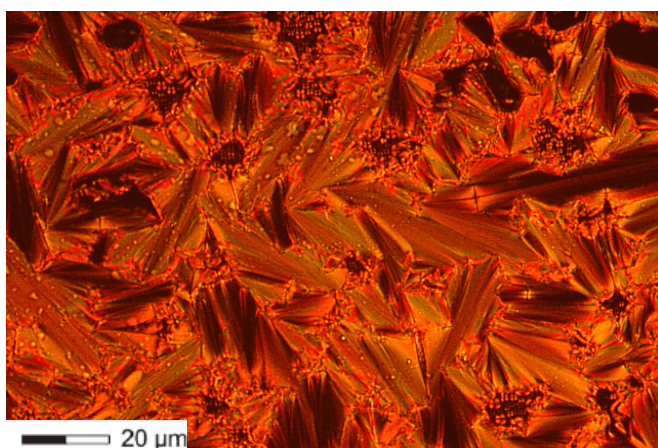

Figure S17: Photomicrographs of the smectic A phase of **Pt(thpyC₁₂)₂** between untreated glass slides obtained by cooling from the isotropic liquid to 145 °C.
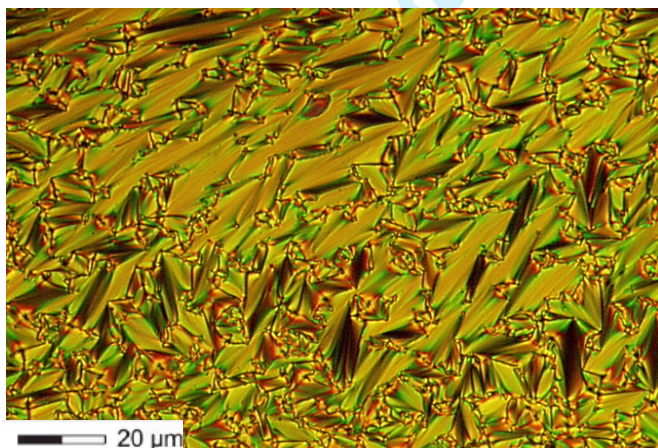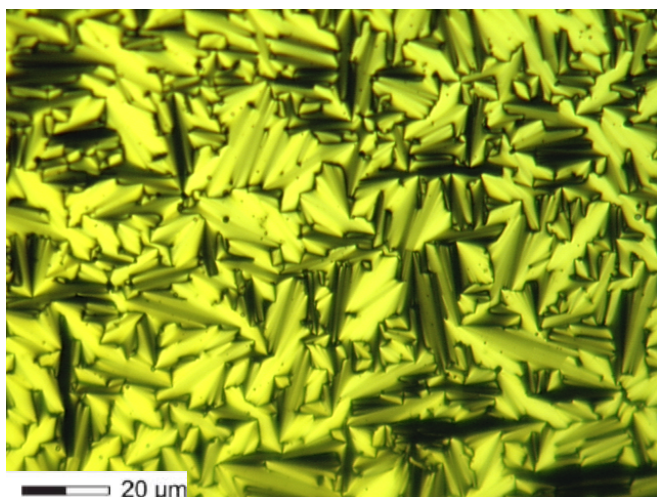

Figure S18: Photomicrographs of the smectic A phase of **Pt(thpyC₁₀)₂** between untreated glass slides obtained by cooling from the isotropic liquid to 158 °C.

Figure S19: Photomicrographs of the smectic A phase of **Pt(thpyC₈)₂** between untreated glass slides obtained by cooling from the isotropic liquid to 166 °C.

Figure S20: Photomicrographs of the smectic A phase of **Pt(thpyC$_{12}$B)$_2$** between untreated glass slides obtained by cooling from the isotropic liquid to 105 °C.
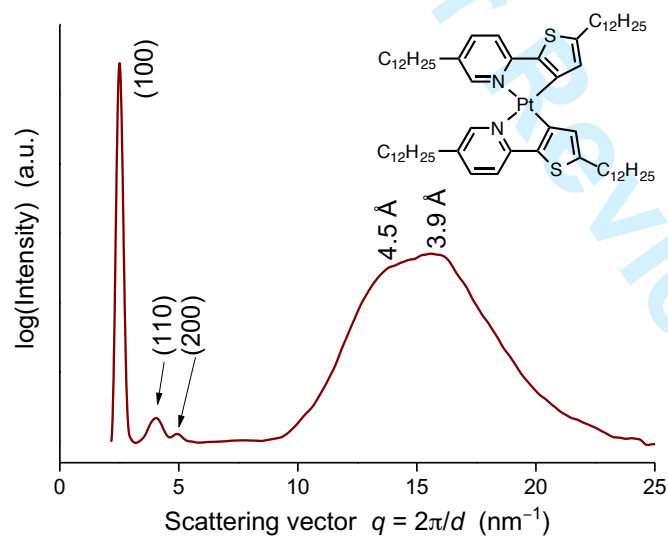
Powder X-Ray Diffraction

Figure S21: Powder X-Ray Diffraction patterns of **Pt(thpyC$_{12}$)$_2$** showing a Col$_h$ ordering at 130 °C. Distances in Å are shown in above each reflection.
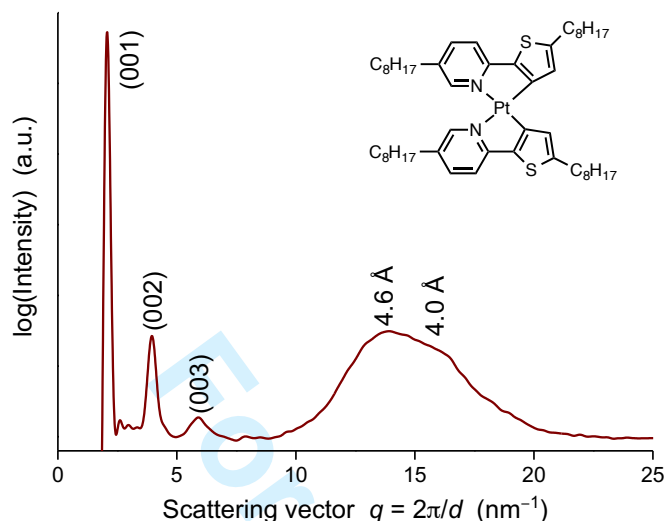
Figure S22: Powder X-Ray Diffraction patterns of **Pt(thpyC₈)₂** showing a SmA ordering at 160 °C. Distances in Å are shown above each reflection.
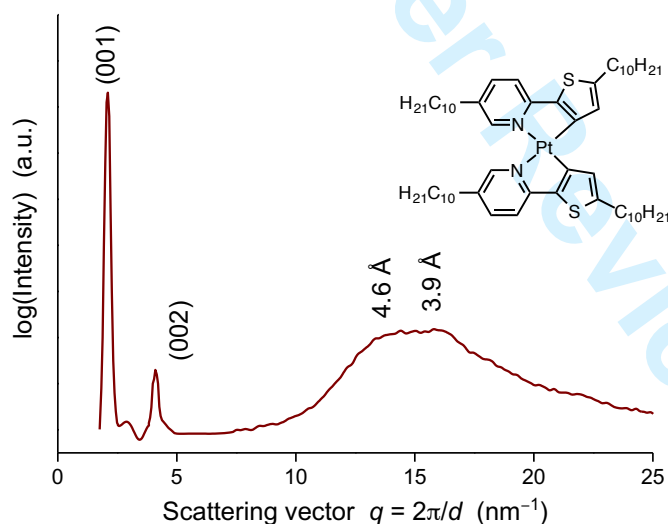

Figure S23: Powder X-Ray Diffraction patterns of **Pt(thpyC₈)₂** showing a SmA ordering at 160 °C. Distances in Å are shown above each reflection.

Single Crystal Diffraction Data

Low-temperature diffraction data (φ-and ω-scans) were collected on a Bruker-AXS X8 Kappa Duo diffractometer coupled to a Smart Apex2 CCD detector with Mo *K*α radiation (λ = 0.71073 Å) from an *IμS* micro-source. Structures were solved by direct methods using SHELXS8[1] and refined against *F2* on all data by full-matrix least squares with SHELXL-97,[2] following established refinement strategies.[3-6] All non-hydrogen atoms were refined anisotropically. All hydrogen atoms were included in the model at geometrically calculated positions and refined using a riding model. The isotropic

displacement parameters of all hydrogen atoms were fixed to 1.2 times the *U* value of the atoms they are linked to (1.5 times for methyl groups).

Crystals were obtained as long needles by slow evaporation of a saturated CH_2Cl_2 solution.
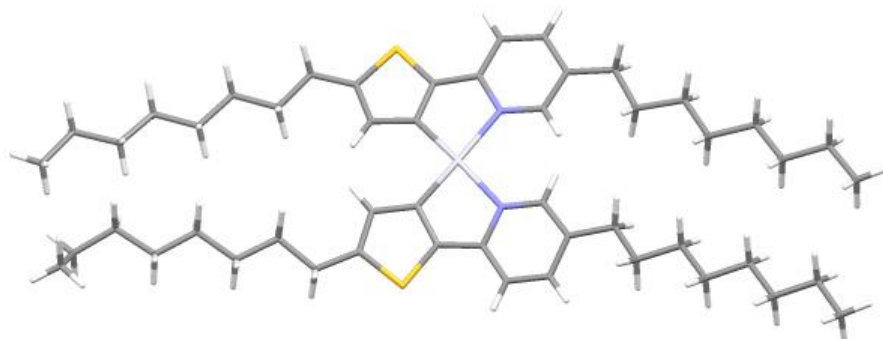

Figure S24: **Pt(thpyC$_8$)$_2$** single crystal structure obtained by recrystallization from DCM.

Table: Crystal data and structure refinement for **Pt(thpyC$_8$)$_2$**

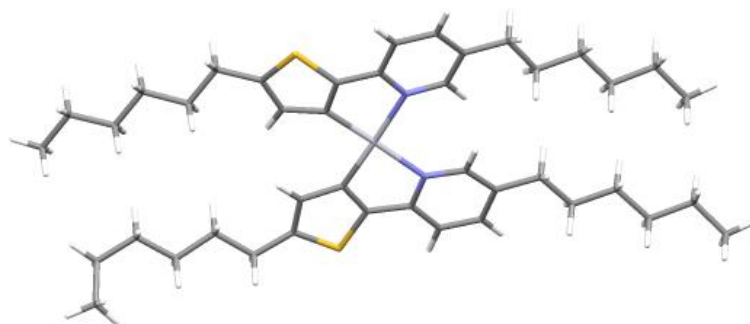| Compound	Pt(thpyC$_8$)$_2$
Empirical formula	$C_{50}H_{76}N_2PtS_2$
Formula weight	964.379
Crystal system	monoclinic
Space group	$P2_1$
Unit cell dimensions	a = 7.7798(5) Å
	b = 20.8106(14) Å
	c = 28.619(2) Å
	$\alpha = 90°$
	$\beta = 97.6462(14)°$
	$\gamma = 90°$
Volume	4592.3(5) Å^3
Temperature	100 K
Z	4
Density (calculated)	1.395 Mg/m^3
Absorption coefficient	3.181 mm^{-1}
F(000)	2000
Crystal size	$0.310 \times 0.290 \times 0.025$ mm^3
Theta range for data collection	1.214 to 30.507˚
Index ranges	-11 ≤ h ≤ 11, -29 ≤ k ≤ 29, -40 ≤ l ≤ 40
Reflections collected	169170
Independent reflections	27969 [R(int) = 0.0514]
Absorption correction	3.181
Goodness-to-fit on F2	1.035
Final R indices [I>2sigma(I)]	0.0525

Figure S25: **Pt(thpyC₆)₂** single crystal structure obtained by recrystallization from DCM

Table: Crystal data and structure refinement for **Pt(thpyC₆)₂**

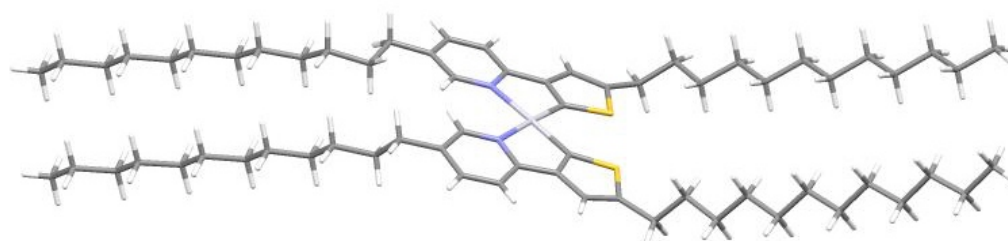| Compound	Pt(thpyC₆)₂
Empirical formula	$C_{42}H_{60}N_2PtS_2$
Formula weight	852.13
Crystal system	monoclinic
Space group	$P2_1/c$
Unit cell dimensions	a = 24.378(2) Å
	b = 7.7398(7) Å
	c = 21.2759(19) Å
	α = 90°
	β = 107.883(2)°
	γ = 90°
Volume	3820.4(6) Å³
Temperature	100 K
Z	4
Density (calculated)	1.482 Mg/m³
Absorption coefficient	3.814 mm⁻¹
F(000)	1744
Crystal size	$0.30 \times 0.15 \times 0.05$ mm³
Theta range for data collection	2.43 to 30.68˚
Index ranges	-33 ≤ h ≤ 33, -10 ≤ k ≤ 10, -29≤ l ≤ 29
Reflections collected	82261
Independent reflections	[R(int) = 0.0336]
Absorption correction	3.814
Goodness-to-fit on F2	1.048
Final R indices [I>2sigma(I)]	0.0385

Figure S26: **Pt(thpyC₁₂B)₂** single crystal structure obtained by recrystallization from DCM.

Table: Crystal data and structure refinement for **Pt(thpyC₁₂B)₂**

| Compound	Pt(thpyC₁₂B)₂
Empirical formula	$C_{66}H_{108}N_2PtS_2$
Formula weight	1188.75
Crystal system	monoclinic
Space group	*P*2₁/c
Unit cell dimensions	a = 35.690(4) Å
	b = 17.6972(18) Å
	c = 9.7953(10) Å
	$\alpha = 90°$
	$\beta = 92.398(2)°$
	$\gamma = 90°$
Volume	6181.4(11) Å³
Temperature	100 K
Z	4
Density (calculated)	1.277 Mg/m³
Absorption coefficient	2.377 mm⁻¹
F(000)	2512
Crystal size	0.20 × 0.20 × 0.04 mm³
Theta range for data collection	2.38 to 30.47˚
Index ranges	-49 ≤ h ≤ 49, -24 ≤ k ≤ 24, -13 ≤ l ≤ 13
Reflections collected	128735
Independent reflections	17348 [R(int) = 0.0617]
Absorption correction	2.377
Goodness-to-fit on F2	1.041
Final R indices [I>2sigma(I)]	0.0599

Photophysical Data
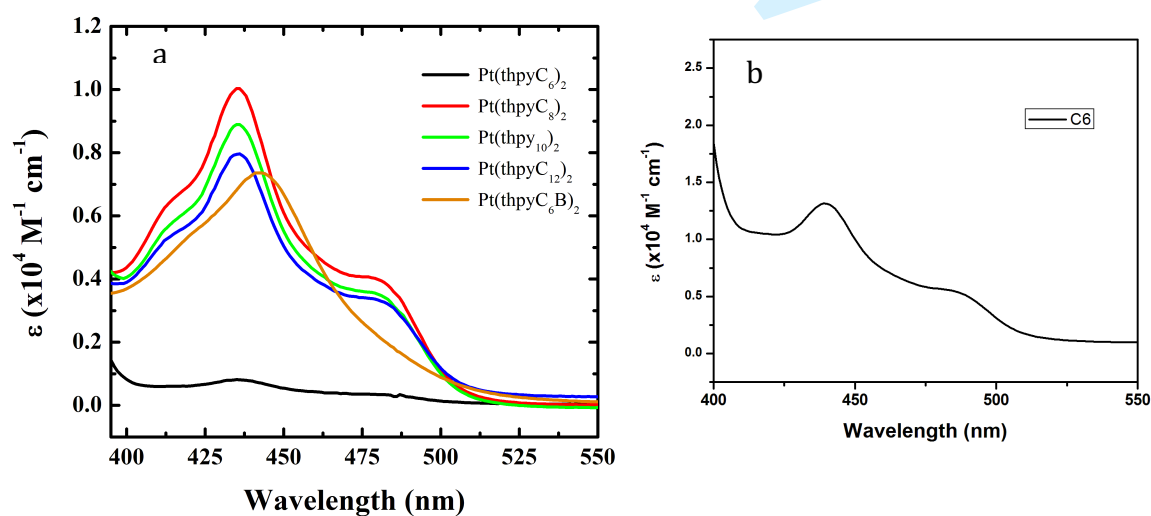
Figure S27: a) UV-vis absorption spectra of the **Pt(thpyR)₂** series in THF (10⁻⁴ M) b) UV-vis absorption spectrum of **Pt(thpyC₆)₂** in 1,2,4-trichlorobenzene (10⁻⁴ M)
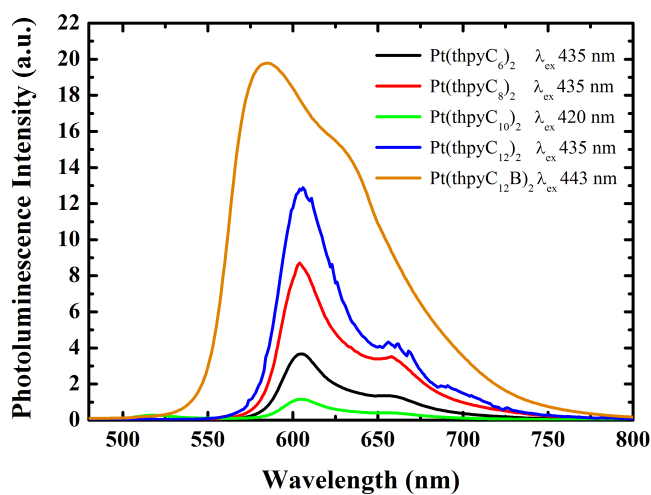
Figure S28: Photoluminescence spectra of the **Pt(thpyR)₂** series in THF (10^{-4} M) at room temperature under Ar
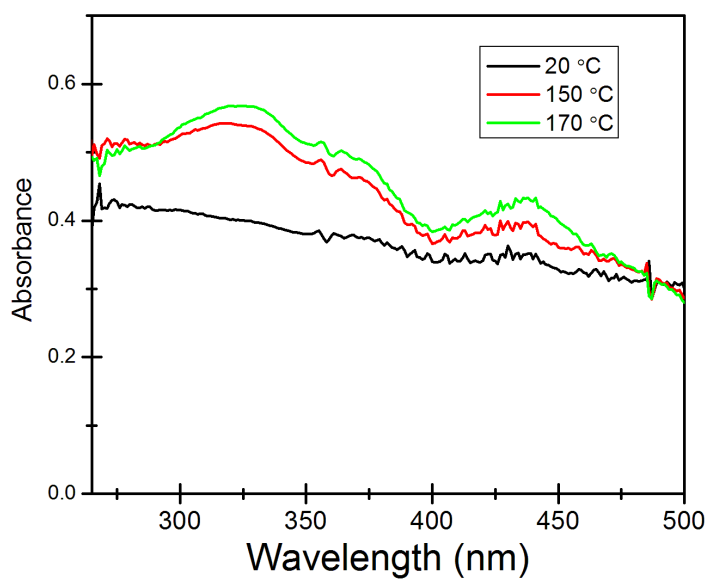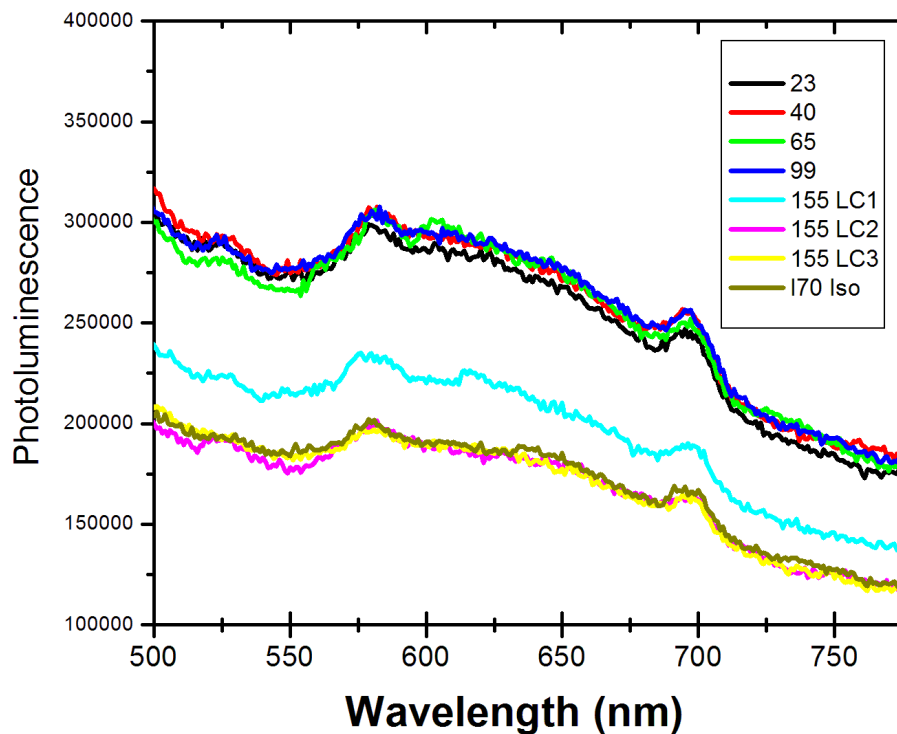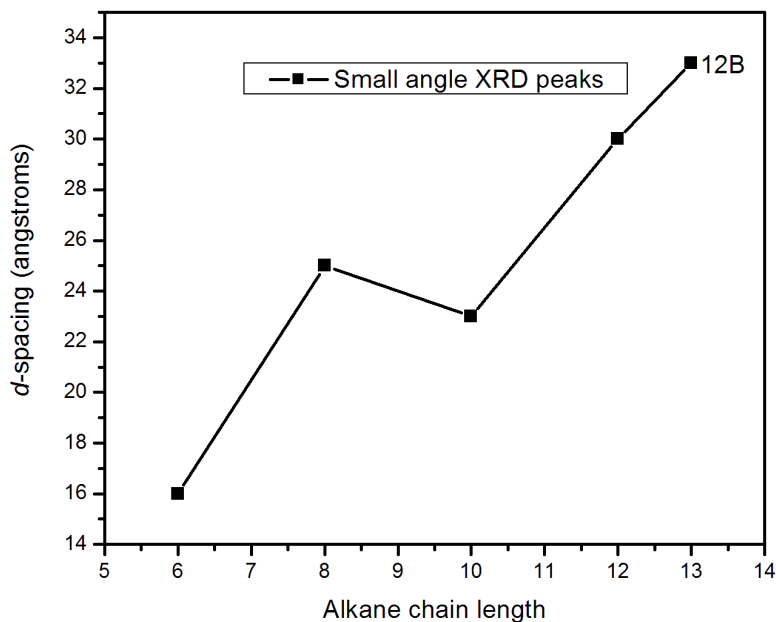

Figure S29: Thin film UV-visible spectra of **Pt(thpyC₈)₂** at room temperature, 150°C, and 170 ˚C, the crystalline, liquid crystalline, and isotropic points, respectively

Figure S30: Thin film luminescence spectra of **Pt(thpyC$_8$)$_2$** at various temperatures (different colored lines in ˚C). LC1 is after 1 minute, LC2 is after 5 mins, and LC3 is after 10 mins of equilibration.

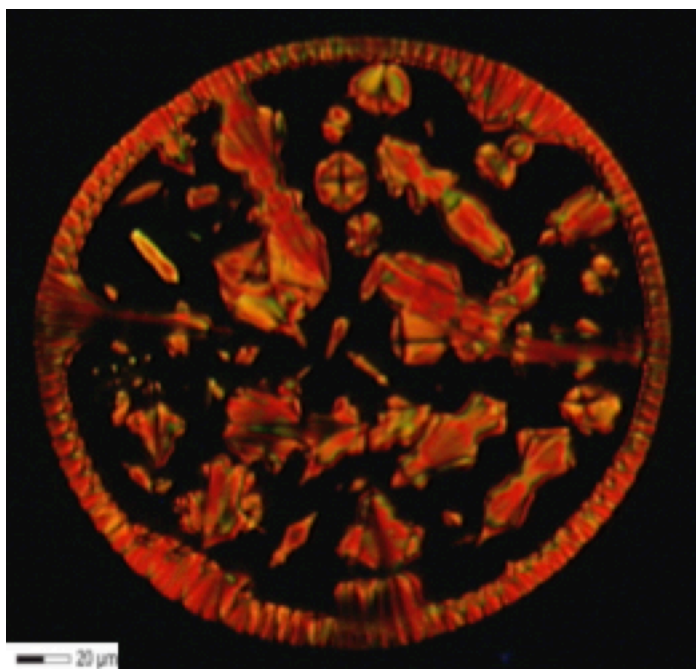Figure S31: *d*-spacing of small angle X-ray diffraction peaks in the mesophase based on alkyl chain length

Figure S32: Polarized optical microscope images of **Pt(thpyC$_{12}$)$_2$** at 114 ˚C with crossed polarizers showing both coexistence of SmA and Col$_h$ mesophases

References

1. Sheldrick, G. M. *Acta Crystallogr., Sect. A* **2007**, *64*, 112–122.
2. Sheldrick, G. M. *Acta Crystallogr., Sect. A* **1990**, *46*, 467–473.
3. Müller, P. *Crystallogr. Rev.* **2009**, *15*, 57–83.
4. Sheldrick, G. M. CELL_NOW; University of Göttingen: Germany, 2007.
5. Bruker SAINT; Bruker-AXS Inc.: Madison, Wisconsin, USA, 2007.
6. Sheldrick, G. M. TWINABS; University of Göttingen: Germany, 2007.